Eur. Phys. J. Plus (2019) **134**: 244
DOI 10.1140/epjp/i2019-12584-3

THE EUROPEAN PHYSICAL JOURNAL PLUS

Regular Article

A high-order split-step finite difference method for the system of the space fractional CNLS

Meng Li[a]

School of Mathematics and Statistics, Zhengzhou University, Zhengzhou 450001, China

Received: 25 July 2018 / Revised: 5 February 2019
Published online: 30 May 2019

Abstract. In this paper, the schemes based on the high-order quasi-compact split-step finite difference methods are derived for the one- and two-dimensional coupled fractional Schrödinger equations. In order to improve the computing efficiency, we adopt the split-step method for handling the nonlinearity. By using a high-order quasi-compact scheme in space, the numerical method improves the accuracy effectively. We prove the conservation laws, prior boundedness and unconditional error estimates of the quasi-compact finite difference scheme for the linear problem. Moreover, for the nonlinear problem, we show that the quasi-compact split-step finite difference method can also keep the conservation law in the mass sense. For solving the multi-dimensional problem, we combine the quasi-compact split-step method with the alternating direction implicit technique. At last, numerical examples are performed to illustrate our theoretical results and show the efficiency of the proposed schemes.

1 Introduction

The fractional Schrödinger equation (FSE), as a natural generalization of the classical (integer order) Schrödinger equation, has been widely exploited to study fractional quantum phenomena. In [1, 2], Laskin extended the Feynman path integral to the Lévy one, and then obtained the FSE including a space fractional derivative of order α ($1 < \alpha < 2$) instead of the Laplacian in the classical Schrödinger equation. Naber [3] derived the time-fractional Schrödinger equation by replacing the first-order time derivative with a Caputo fractional derivative. We can find more physical applications of the FSE in [2, 4–9]. The extensive theoretical studies, such as the well-posedness, conservation law, dynamics and ground states of the FSEs, can be found in [2, 3, 10–13]. From the numerical point of view, Amore *et al.* [14] developed a collocation method to obtain the numerical solutions to the quantum-mechanical problems involving a fractional Laplacian. Bao and Dong [15] constructed a time-splitting sine pseudospectral method for the nonlinear relativistic Hartree equation. In [16], Atangana *et al.* solved the space fractional variable-order Schrödinger equation numerically via the Crank-Nicolson scheme, and then presented the stability and the convergence results. Wei *et al.* [17,18] considered implicit fully discrete local discontinuous Galerkin methods for the time FSEs. Zhao *et al.* [19] proposed a novel fourth-order compact ADI scheme for two-dimensional nonlinear space FSE. In [20–22], a series of efficient numerical schemes were constructed for the coupled nonlinear FSEs with the Riesz fractional derivative. Wang and Huang [23–26] studied the nonlinear FSEs via various finite difference methods. Li *et al.* [27–30] derived the numerical solutions of the nonlinear FSE by using some difference schemes in time and finite-element methods in space. In [31], Bhrawy *et al.* put forward an improved a collocation method for multi-dimensional space-time variable-order FSEs. There were also some other numerical methods dealing with the classical Schrödinger equations and fractional problems, such as [32–40].

As we all know, due to the efficiency in saving CPU time computer memory, the splitting methods are widely adopted in many nonlinear problems. In the earlier work, Weideman [41] pointed an efficient and stable split-step method for the numerical solution of the nonlinear Schrödinger equation. Muslu *et al.* [42] numerically solved the generalized nonlinear Schrödinger equation by a split-step Fourier method. Wang [43] utilized the split-step finite difference method to solve various types of nonlinear Schrödinger equations. Taha *et al.* [44] introduced a parallel split-step Fourier method to numerically solve the coupled nonlinear Schrödinger equation and presented some numerical experiments to show that the methods have accurate results and considerable speedup.

[a] e-mail: limeng@zzu.edu.cn

In order to improve the spatial accuracy, there are also the authors using the high-order compact split-step finite difference scheme to numerically solve the nonlinear Schrödinger equations [45–49]. The success of the split-step method for the classical nonlinear Schrödinger equations, prompted several authors to try to extend this method to the FSE. Wang and Huang [26] constructed a split-step alternating direction implicit difference scheme for solving the FSEs in two dimensions. In [50], Duo and Zhang proposed three Fourier spectral methods for the FSEs, including the split-step Fourier spectral method, the Crank-Nicolson Fourier spectral method and the relaxation Fourier spectral method. In [51], the split-step quasi-compact finite difference method was proposed to solve the nonlinear fractional Ginzburg-Landau equations both in one and two dimensions. However, there is no work focusing on the high-order (quasi-)compact split-step difference method for the space fractional coupled nonlinear Schrödinger equation (CNLS).

In this paper, we consider a high-order quasi-compact split-step difference method for the system of the space fractional CNLS ($1 < \alpha \leq 2$)

$$iu_t - \kappa(-\Delta)^{\frac{\alpha}{2}}u + \rho(|u|^2 + \beta|v|^2)u = 0, \quad x \in \mathbb{R},\ t > 0, \tag{1}$$

$$iv_t - \kappa(-\Delta)^{\frac{\alpha}{2}}v + \rho(|v|^2 + \beta|u|^2)v = 0, \quad x \in \mathbb{R},\ t > 0, \tag{2}$$

with the initial conditions

$$u(x,0) = u_0(x), \quad v(x,0) = v_0(x), \quad x \in \mathbb{R}, \tag{3}$$

where $i = \sqrt{-1}$ is the complex unit, $u(x,t)$ and $v(x,t)$ are two complex-valued wave functions of time t and space x, κ, ρ and β are positive real constants, and $u_0(x)$ and $v_0(x)$ are given complex-valued smooth initial data. The operator $(-\Delta)^{\alpha/2}$ is defined by

$$-(-\Delta)^{\alpha/2}u(x,t) := -\frac{1}{2\cos(\alpha\pi/2)}({}_{-\infty}D_x^{\alpha} + {}_xD_{+\infty}^{\alpha})u(x,t), \tag{4}$$

where ${}_{-\infty}D_x^{\alpha}u(x,t)$ denotes the left-side Riemann-Liouville fractional derivative

$${}_{-\infty}D_x^{\alpha}u(x,t) = \frac{1}{\Gamma(2-\alpha)}\frac{\mathrm{d}^2}{\mathrm{d}x^2}\int_{-\infty}^{x}\frac{u(\xi,t)}{(x-\xi)^{\alpha-1}}\mathrm{d}\xi,$$

and ${}_xD_{+\infty}^{\alpha}u(x,t)$ denotes the right-side Riemann-Liouville fractional derivative

$${}_xD_{+\infty}^{\alpha}u(x,t) = \frac{1}{\Gamma(2-\alpha)}\frac{\mathrm{d}^2}{\mathrm{d}x^2}\int_{x}^{+\infty}\frac{u(\xi,t)}{(\xi-x)^{\alpha-1}}\mathrm{d}\xi.$$

Following a similar approach as [11, 15, 45, 52], we easily obtain the following two standard conserved quantities (mass and energy) for the space fractional CNLS (1)–(3).

Proposition 1. *If the wave functions $u(x,t)$ and $v(x,t)$ are the solutions of* (1)–(3)*, then we have the following conservation results:*

1) *mass conservation:*

$$M_1(t) \equiv M_1(0), \quad M_2(t) \equiv M_2(0), \quad t > 0, \tag{5}$$

2) *energy conservation:*

$$E(t) \equiv E(0), \quad t > 0, \tag{6}$$

where $M_1(t) := \|u\|^2_{L^2(\mathbb{R})}$, $M_2(t) := \|v\|^2_{L^2(\mathbb{R})}$, $E(t) := \frac{\kappa}{2}(\|(-\Delta)^{\frac{\alpha}{4}}u\|^2_{L^2(\mathbb{R})} + \|(-\Delta)^{\frac{\alpha}{4}}v\|^2_{L^2(\mathbb{R})}) - \frac{\rho}{4}(\|u\|^4_{L^4(\mathbb{R})} + \|v\|^4_{L^4(\mathbb{R})} + 2\beta\int_{\mathbb{R}}|u|^2|v|^2\mathrm{d}x)$. Here, $\|\cdot\|_{L^2(\mathbb{R})}$ and $\|\cdot\|_{L^4(\mathbb{R})}$ denote the L^2-norm and L^4-norm, respectively.

Proof. Computing the inner product of u and v with (1) and (2) respectively, and then taking the imagine parts of the resulting equations, we can immediately obtain (5). Moreover, computing the inner product of u_t and v_t with (1) and (2), respectively, and then taking the real parts of the resulting equations, we can also derive (6). □

The above conservation properties of the exact solutions $u(x,t)$ and $v(x,t)$ also motivate us to study the conservation results along the numerical front. As we all know, the conservative schemes perform better than the nonconservative ones for the classical Schrödinger equation. In [53], Zhang *et al.* proposed that the nonconservative schemes may easily show their nonlinear blow-up. Li and Vu-Quoc [54] pointed out that one of the criterions to judge the success of a numerical simulation was the ability to preserve some invariant properties of the original differential equation. For the FSEs, there have been a lot of numerical methods satisfying the conservation properties. For example, the schemes in [20, 24] are mass conservative, and the schemes in [21–23, 25, 27, 55] satisfy both the mass and energy conservation.

All these schemes show their advantages in the long-time simulation. Nevertheless, to the best of our knowledge, there is no work to utilize the high-order quasi-compact split-step difference scheme to study the conservation properties of the space fractional CNLS.

This paper is organized as follows. In sect. 2, we introduce the quasi-compact WSGD operator for discretizing the Riesz fractional derivatives, and the definitions and properties of the fractional Sobolev norm. In sect. 3, the quasi-compact split-step WSGD scheme is derived for the fractional CNLS. In sect. 4, the rigorous theoretical analysis, including the conservation laws, prior boundedness and unconditional error estimates, are given for the difference scheme of the linear problem. Moreover, we show in this section that the constructed quasi-compact split-step difference scheme of the nonlinear problem can also keep the conservation law in the mass sense. For the multi-dimensional system, we derive a quasi-compact ADI split-step difference method in sect. 6. In sect. 7, numerical examples are performed to check our theoretical results and show the efficiency of the proposed schemes. Some conclusions are drawn in sect. 8, and some other three difference schemes in two dimensions are introduced in sect. A for the demand of the experiment.

2 Preliminaries

2.1 Quasi-compact WSGD operator for Riesz fractional derivatives

Various numerical methods have been given for approximating the Riemann-Liouville fractional derivative, such as the first-order accuracy shifted Grünwald scheme [56,57], second-order accurate weighted and shifted Grünwald difference scheme [58], high-order difference algorithms [59–63]. The shifted Grünwald formulae is defined by [56]

$$ {}_L\mathscr{A}^{\alpha}_{h,p}u(x) := \frac{1}{h^{\alpha}}\sum_{l=0}^{\infty} g_l^{(\alpha)}u(x-(l-p)h) = {}_{-\infty}D^{\alpha}_x u(x) + O(h), \tag{7a} $$

$$ {}_R\mathscr{A}^{\alpha}_{h,p}u(x) := \frac{1}{h^{\alpha}}\sum_{l=0}^{\infty} g_l^{(\alpha)}u(x+(l-r)h) = {}_xD^{\alpha}_{+\infty} u(x) + O(h), \tag{7b} $$

where p, r are integers and g_l^{α} $(l \geq 0)$ are the coefficients of the power series of $(1-z)^{\alpha}$, such that

$$ (1-z)^{\alpha} = \sum_{l=0}^{\infty}(-1)^l\binom{\alpha}{l}z^l = \sum_{l=0}^{\infty} g_l^{(\alpha)}z^l, \quad |z|<1. \tag{8} $$

Obviously, the coefficients $\{g_l^{\alpha}\}$ can be computed by the following recursive form:

$$ g_0^{(\alpha)} = 1, \quad g_l^{(\alpha)} = \left(1-\frac{\alpha+1}{l}\right)g_{l-1}^{(\alpha)}, \quad l = 1,2,\ldots. $$

The weighted and shifted Grünwald difference (WSGD) operators are then given by [63]

$$ \begin{aligned} {}_L\mathscr{D}^{\alpha}_h u(x) &= \lambda_1 {}_L\mathscr{A}^{\alpha}_{h,1}u(x) + \lambda_0 {}_L\mathscr{A}^{\alpha}_{h,0}u(x) + \lambda_{-1} {}_L\mathscr{A}^{\alpha}_{h,-1}u(x), \\ {}_R\mathscr{D}^{\alpha}_h u(x) &= \lambda_1 {}_R\mathscr{A}^{\alpha}_{h,1}u(x) + \lambda_0 {}_R\mathscr{A}^{\alpha}_{h,0}u(x) + \lambda_{-1} {}_R\mathscr{A}^{\alpha}_{h,-1}u(x), \end{aligned} \tag{9} $$

where

$$ \lambda_1 = \frac{\alpha^2+3\alpha+2}{12}, \qquad \lambda_0 = \frac{4-\alpha^2}{6}, \qquad \lambda_{-1} = \frac{\alpha^2-3\alpha+2}{12}. $$

Therefore, rearranging the WSGD operators obtains that

$$ {}_L\mathscr{D}^{\alpha}_h u(x) = \frac{1}{h^{\alpha}}\sum_{l=0}^{\infty} w_l^{(\alpha)}u(x-(l-1)h), \qquad {}_R\mathscr{D}^{\alpha}_h u(x) = \frac{1}{h^{\alpha}}\sum_{l=0}^{\infty} w_l^{(\alpha)}u(x+(l-1)h), \tag{10} $$

where the coefficients $w_i^{(\alpha)}$ $(i \geq 0)$ are defined by

$$ w_0^{(\alpha)} = \lambda_1 g_0^{(\alpha)}, \quad w_1^{(\alpha)} = \lambda_1 g_1^{(\alpha)} + \lambda_0 g_0^{(\alpha)}, \quad w_l^{(\alpha)} = \lambda_1 g_l^{(\alpha)} + \lambda_0 g_{l-1}^{(\alpha)} + \lambda_{-1} g_{l-2}^{(\alpha)} \quad (l \geq 2). \tag{11} $$

Lemma 1. (*See* [63,64].) *The coefficients* $w_i^{(\alpha)}$ $(i \geq 0)$ *have the properties*

$$ \begin{cases} w_0^{(\alpha)} \geq 0, \quad w_1^{(\alpha)} \geq 0, \quad w_l^{(\alpha)} \geq 0, \quad l \geq 3, \\ \displaystyle\sum_{l=0}^{+\infty} w_l^{(\alpha)} = 0, \quad \sum_{l=0}^{M} w_l^{(\alpha)} \leq 0, \quad M \geq 1, \\ w_0^{(\alpha)} + w_2^{(\alpha)} \geq 0. \end{cases} \tag{12} $$

When $1 < \alpha < 2$, the inequalities in (12) are strictly true, i.e., the sign "$\leq$" and "$\geq$" can be substituted by "$<$" and "$>$".

The quasi-compact operator is defined by

$$\mathcal{A}_x^\alpha u(x) := (I + d_\alpha h^2 \delta_x^2) u(x), \tag{13}$$

where I is the identity operator, $d_\alpha = (-\alpha^2 + \alpha + 4)/24$ and

$$\delta_x^2 u(x) = \frac{u(x-h) + u(x) + u(x+h)}{h^2}.$$

The following lemma gives the error estimates between the Riemann Liouville derivatives and the quasi-compact WSGD operators.

Lemma 2. (*See* [63].) *Suppose that $u \in L^1(\mathbb{R})$ and*

$$u(x) \in \mathscr{C}^{4+\alpha}(\mathbb{R}) := \left\{ u \middle| \int_{-\infty}^{+\infty} (1+|\xi|)^{4+\alpha} |\hat{u}(\xi)| \mathrm{d}\xi < \infty \right\},$$

where $\hat{u}(\xi)$ is the Fourier transformation of $u(x)$. Then for a fixed h, the quasi-compact operators hold

$${}_L\mathscr{D}_h^\alpha u(x) := \mathcal{A}_x^\alpha ({}_{-\infty}D_x^\alpha u(x)) + O(h^4), \qquad {}_R\mathscr{D}_h^\alpha u(x) := \mathcal{A}_x^\alpha ({}_xD_{+\infty}^\alpha u(x)) + O(h^4),$$

uniformly for $x \in \mathbb{R}$. Particularly, if $\alpha = 2$, then it coincides with the approximation of the second-order derivative.

Define

$$\begin{aligned} \Delta_h^\alpha u(x) &:= \frac{1}{2\cos\frac{\alpha\pi}{2}} \left({}_L\mathscr{D}_h^\alpha u(x) + {}_R\mathscr{D}_h^\alpha u(x) \right) \\ &= \frac{1}{h^\alpha} \frac{1}{2\cos\frac{\alpha\pi}{2}} \left(\sum_{l=0}^{\infty} w_l^{(\alpha)} u(x-(l-1)h) + \sum_{l=0}^{\infty} w_l^{(\alpha)} u(x+(l-1)h) \right). \end{aligned} \tag{14}$$

From lemma 2, we have

$$\Delta_h^\alpha u(x) = \mathcal{A}_x^\alpha ((-\Delta)^{\frac{\alpha}{2}} u(x)) + O(h^4), \quad u(x) \in L^1(\mathbb{R}) \cap \mathscr{C}^{4+\alpha}(\mathbb{R}). \tag{15}$$

It is remarkable that when we replace the quasi-compact $\mathcal{A}_x^\alpha$ by the identity operator I, we have

$$\Delta_h^\alpha u(x) = (-\Delta)^{\frac{\alpha}{2}} u(x) + O(h^2), \quad u(x) \in L^1(\mathbb{R}) \cap \mathscr{C}^{2+\alpha}(\mathbb{R}). \tag{16}$$

2.2 Fractional Sobolev norm

Denote $h\mathbb{Z}$ be the infinite grid with the gird points $x_j = jh$ for $j \in \mathbb{Z}$. For any grid functions $u = \{u_j\}$ and $\omega = \{\omega_j\}$ on $h\mathbb{Z}$, we define the discrete inner product and its associated l_h^2 norm as

$$(u, v) = h \sum_{j \in \mathbb{Z}} u_j \bar{v}_j, \quad \|u\|^2 = (u, u),$$

where $\bar{v}$ denotes the conjugate of v. Furthermore, the discrete l^p norms are defined by

$$\|u\|_{l^p}^p = h \sum_{j \in \mathbb{Z}} |u_j|^p \quad (1 \leq p < +\infty), \quad \|u\|_{l^\infty} = \sup_{j \in \mathbb{Z}} |u_j|.$$

For any $u \in l_h^2 := \{u \mid u = \{u_j\},\ \|u\|_h < +\infty,\ j \in \mathbb{Z}\}$, denote $\hat{u} \in L^2[-\pi/h, \pi/h]$ be the semi-discrete Fourier transform of u, *i.e.*,

$$\hat{u}(k) := \frac{1}{\sqrt{2\pi}} h \sum_{j \in \mathbb{Z}} u_j e^{-ikx_j}$$

(see [65,66]). Obviously,

$$u_j = \frac{1}{\sqrt{2\pi}} \int_{-\pi/h}^{\pi/h} \hat{u}(k) e^{ikx_j} \mathrm{d}k.$$

By using Parseval's theorem, we have

$$(u,w)_h=\int_{-\pi/h}^{\pi/h}\hat{u}(k)\overline{\hat{w}(k)}\mathrm{d}k.$$

Define the fractional Sobolev semi-norm and norm as follows:

$$|u|_{H^\mu}^2=\int_{-\pi/h}^{\pi/h}|k|^{2\mu}|\hat{u}(k)|^2\mathrm{d}k,\qquad \|u\|_{H^\mu}^2=\|u\|^2+|u|_{H^\mu}^2. \tag{17}$$

We now introduce the following two lemmas, which play the essential role in the subsequent theoretical analysis [52].

Lemma 3. (*Discrete Sobolev inequality.*) *For any* $1/2<\mu\le 1$*, there exists a constant* $C_\mu=C(\mu)>0$*, such that*

$$\|u\|_{l^\infty}\le C_\mu\|u\|_{H^\mu}. \tag{18}$$

Lemma 4. *For any* $1<\alpha\le 2$*, we have*

$$C_\alpha|u|_{H^{\frac{\alpha}{2}}}^2\le(\Delta_h^\alpha u,u)\le|u|_{H^{\frac{\alpha}{2}}}^2, \tag{19}$$

where $C_\alpha=\frac{2^\alpha(1-\alpha^2)}{3\pi^\alpha\cos\frac{\alpha\pi}{2}}>0$.

3 Derivation of a quasi-compact split-step WSGD scheme

In practical computation, if $u(x,t)$ and $v(x,t)$ are defined on the finite interval $\Omega=(a,b)$ and satisfy the homogeneous boundary conditions, we can extend the functions by taking $u(x,t)\equiv 0$ and $v(x,t)\equiv 0$ for $x\le a$ and $x\ge b$, respectively. Therefore, the space fractional CNLS (1)–(3) is truncated as

$$iu_t-\kappa(-\Delta)^{\frac{\alpha}{2}}u+\rho(|u|^2+\beta|v|^2)u=0,\quad (x,t)\in\Omega\times(0,T], \tag{20}$$
$$iv_t-\kappa(-\Delta)^{\frac{\alpha}{2}}v+\rho(|v|^2+\beta|u|^2)v=0,\quad x\in\Omega\times(0,T], \tag{21}$$
$$u(x,0)=u_0(x),\quad v(x,0)=v_0(x),\quad x\in\Omega, \tag{22}$$
$$u(x,t)=0,\quad v(x,t)=0,\quad x\in\mathbb{R}\backslash\Omega,\quad t\in[0,T], \tag{23}$$

where, under the homogeneous boundary conditions, the Riesz fractional derivative has reduced to

$$-(-\Delta)^{\frac{\alpha}{2}}u(x,t)=-\frac{1}{2\cos\frac{\alpha\pi}{2}}[{}_aD_x^\alpha u(x,t)+{}_xD_b^\alpha u(x,t)].$$

The boundary conditions (23) are referred to as the nonlocal volume constraint (or the extended Dirichlet boundary) and the corresponding problem (20)–(23) as the volume constraint problem (see [67,68]).

Let M, N be any positive integers and $h=(b-a)/M$, $\tau=T/N$. We define a partition of $[0,T]\times[a,b]$ by $\Omega_\tau\times\Omega_h$ with the grid $\Omega_\tau=\{t_n=n\tau;\ n=0,1,\cdots,N\}$ and $\Omega_h=\{x_j=a+jh;\ j=0,1,\cdots,M\}$. From (10), if $u\in\mathscr{C}^{4+\alpha}(\mathbb{R})$ (see remark 2.5 in [63]), we have the simplified WSGD operator

$${}_L\mathscr{D}_h^\alpha u(x):=\frac{1}{h^\alpha}\sum_{l=0}^{j+1}w_l^{(\alpha)}u(x_{j-l+1})={}_aD_x^\alpha u(x)+O(h^2), \tag{24a}$$

$${}_R\mathscr{D}_h^\alpha u(x):=\frac{1}{h^\alpha}\sum_{l=0}^{M-j+1}w_l^{(\alpha)}u(x_{j+l-1})={}_xD_b^\alpha u(x)+O(h^2). \tag{24b}$$

Then, we get the following WSGD approximation of the Riesz fractional derivative

$$\begin{aligned}\Delta_h^\alpha u(x)&=\frac{1}{2\cos\frac{\alpha\pi}{2}}({}_L\mathscr{D}_h^\alpha u(x)+{}_R\mathscr{D}_h^\alpha u(x))\\&=\frac{1}{h^\alpha}\frac{1}{2\cos\frac{\alpha\pi}{2}}\left(\sum_{l=0}^{j+1}w_l^{(\alpha)}u(x_{j-l+1})+\sum_{l=0}^{M-j+1}w_l^{(\alpha)}u(x_{j+l-1})\right)\\&=\mathcal{A}_x^\alpha((-\Delta)^{\frac{\alpha}{2}}u(x))+O(h^4),\end{aligned} \tag{25}$$

Given any sequence of grid function $\varphi = \{\varphi_j^n \mid (x_j, t_n) \in \Omega_h \times \Omega_\tau\}$, we denote

$$\delta_t \varphi_j^{n+\frac{1}{2}} = \frac{\varphi_j^{n+1} - \varphi_j^n}{\tau}, \qquad \varphi_j^{n+\frac{1}{2}} = \frac{\varphi_j^{n+1} + \varphi_j^n}{2}.$$

For convenience, we denote the index set $\mathcal{T}_M = \{j \mid j = 1, 2, \cdots, M-1\}$ and the grid function space $\mathcal{V}_h = \{\varphi \mid \varphi = (\varphi_1, \varphi_2, \cdots, \varphi_{M-1})\}$. Moreover, under the boundary constraint (23), the previously defined norms are now restricted in $\mathcal{T}_M$.

With these premises, we intend to derive the high-order quasi-compact split-step difference scheme of the space fractional CNLS (20)–(23). To this end, we first split (20) and (21) into linear equations,

$$u_t = Lu(x,t) = -i\kappa(-\Delta)^{\frac{\alpha}{2}} u, \qquad v_t = Lv(x,t) = -i\kappa(-\Delta)^{\frac{\alpha}{2}} v, \tag{26}$$

and nonlinear equations,

$$u_t = N_1(u,v) = i\rho(|u|^2 + \beta|v|^2)u, \qquad v_t = N_2(u,v) = i\rho(|v|^2 + \beta|u|^2)v. \tag{27}$$

We will solve the linear equations (26) by the quasi-compact difference method in space and Crank-Nicolson scheme in time. For the nonlinear equations (27), they can be integrated exactly in the physical space.

Considering (26) on the grid points x_j ($j \in \mathcal{T}_M$), and taking the quasi-compact operator $\mathcal{A}_x^\alpha$ on both sides of the resulting equations give

$$\mathcal{A}_x^\alpha u_t(x_j,t) = \mathcal{A}_x^\alpha (Lu(x_j,t)) = -i\kappa \mathcal{A}_x^\alpha ((-\Delta)^{\frac{\alpha}{2}} u(x_j,t)) \tag{28}$$

and

$$\mathcal{A}_x^\alpha v_t(x_j,t) = \mathcal{A}_x^\alpha (Lv(x_j,t)) = -i\kappa \mathcal{A}_x^\alpha ((-\Delta)^{\frac{\alpha}{2}} v(x_j,t)). \tag{29}$$

By virtue of (15), we have

$$\mathcal{A}_x^\alpha u_t(x_j,t) = -i\kappa \Delta_h^\alpha u(x_j,t) + O(h^4), \qquad \mathcal{A}_x^\alpha v_t(x_j,t) = -i\kappa \Delta_h^\alpha v(x_j,t) + O(h^4). \tag{30}$$

Denote grid functions $U_j^n := u(x_j, t_n)$ ($j \in \mathcal{T}_M,\ 0 \le n \le N$). Then, by using Taylor's expansion, we get

$$u_t(x_j, t_{n+\frac{1}{2}}) = \delta_t U_j^{n+\frac{1}{2}} + O(\tau^2), \qquad \Delta_h^\alpha U_j^{n+\frac{1}{2}} = \frac{\Delta_h^\alpha U_j^{n+1} + \Delta_h^\alpha U_j^n}{2} + O(\tau^2). \tag{31}$$

Hence, taking $t = t_{n+\frac{1}{2}}$ in (28) and utilizing (31) give

$$\mathcal{A}_x^\alpha \delta_t U_j^{n+\frac{1}{2}} = -i\kappa \Delta_h^\alpha \hat{U}_j^{n+\frac{1}{2}} + R_j^{n+\frac{1}{2}}, \tag{32}$$

where $\hat{U}_j^{n+\frac{1}{2}} := (U_j^{n+1} + U_j^n)/2$ and $|R_j^{n+\frac{1}{2}}| = \mathcal{O}(\tau^2 + h^4)$. Similarly, we have

$$\mathcal{A}_x^\alpha \delta_t V_j^{n+\frac{1}{2}} = -i\kappa \Delta_h^\alpha \hat{V}_j^{n+\frac{1}{2}} + P_j^{n+\frac{1}{2}}, \tag{33}$$

in which $|P_j^{n+\frac{1}{2}}| = \mathcal{O}(\tau^2 + h^4)$.

Let u_j^n and v_j^n be the approximation of $u(x_j, t_n)$ and $v(x_j, t_n)$. Then, omitting the truncation errors $R_j^{n+\frac{1}{2}}$ and $P_j^{n+\frac{1}{2}}$ in (32) and (33) respectively, the quasi-compact difference schemes of the linear equations (26) read

$$\mathcal{A}_x^\alpha \delta_t u_j^{n+\frac{1}{2}} + i\kappa \Delta_h^\alpha u_j^{n+\frac{1}{2}} = 0, \quad j \in \mathcal{T}_M, \quad 0 \le n \le N-1, \tag{34}$$

$$\mathcal{A}_x^\alpha \delta_t v_j^{n+\frac{1}{2}} + i\kappa \Delta_h^\alpha v_j^{n+\frac{1}{2}} = 0, \quad j \in \mathcal{T}_M, \quad 0 \le n \le N-1, \tag{35}$$

$$u_j^0 = u_0(x_j), \quad v_j^0 = v_0(x_j), \quad j \in \mathcal{T}_M, \tag{36}$$

$$u_j^n = 0, \quad v_j^n = 0, \quad j \in \mathbb{Z} \backslash \mathcal{T}_M, \quad 0 \le n \le N. \tag{37}$$

Algorithms. The quasi-compact split-step finite difference (SSFD) method for the space fractional CNLS (20)–(23) from time t_n to time t_{n+1}.

Step 1: for $j = 0(1)M$

$$u_j^{n(1)} = \exp\left\{i\rho\left(|u_j^n|^2 + \beta|v_j^n|^2\right)\tau/2\right\} u_j^n, \tag{38}$$

$$v_j^{n(1)} = \exp\left\{i\rho\left(|v_j^n|^2 + \beta|u_j^n|^2\right)\tau/2\right\} v_j^n, \tag{39}$$

Step 2: for $j = 1(1)M-1$

$$\frac{\mathcal{A}_x^\alpha u_j^{n(2)} - \mathcal{A}_x^\alpha u_j^{n(1)}}{\tau} + i\kappa \frac{\Delta_h^\alpha u_j^{n(2)} + \Delta_h^\alpha u_j^{n(1)}}{2} = 0, \tag{40}$$

$$\frac{\mathcal{A}_x^\alpha v_j^{n(2)} - \mathcal{A}_x^\alpha v_j^{n(1)}}{\tau} + i\kappa \frac{\Delta_h^\alpha v_j^{n(2)} + \Delta_h^\alpha v_j^{n(1)}}{2} = 0. \tag{41}$$

Step 3: for $j = 0(1)M$

$$u_j^{n+1} = \exp\left\{ i\rho \left(\left| u_j^{n(2)} \right|^2 + \beta \left| v_j^{n(2)} \right|^2 \right) \tau/2 \right\} u_j^{n(2)}, \tag{42}$$

$$v_j^{n+1} = \exp\left\{ i\rho \left(\left| v_j^{n(2)} \right|^2 + \beta \left| u_j^{n(2)} \right|^2 \right) \tau/2 \right\} v_j^{n(2)}. \tag{43}$$

4 Theoretical properties of the quasi-compact difference scheme

In this section, we show the theoretical analysis of the quasi-compact difference scheme (34)–(37), including the discrete conservation laws, uniform boundedness and optimal higher order error estimate. To this end, We first give the following properties of the operators $\mathcal{A}_x^\alpha$ and Δ_h^α that are needed hereafter.

Lemma 5. (*See* [63].) *$\mathcal{A}_x^\alpha$ is self-adjoint, i.e., for any $u, v \in \mathscr{V}_h$, it holds that*

$$(\mathcal{A}_x^\alpha u, v) = (u, \mathcal{A}_x^\alpha v).$$

Lemma 6. (*See* [63].) *For any $u \in \mathscr{V}_h$, it holds that*

$$\frac{1}{3}\|u\|^2 \le \|u\|_A^2 \le \|u\|^2,$$

where $\|u\|_A := \sqrt{(\mathcal{A}_x^\alpha u, u)}$.

Lemma 7. (*See* [64].) *For any two grid functions $u, v \in \mathscr{V}_h$, there exists a linear operator Λ^α such that*

$$(\Delta_h^\alpha u, v) = (\Lambda^\alpha u, \Lambda^\alpha v).$$

We define below $\mathrm{Im}(s)$ and $\mathrm{Re}(s)$ as the imaginary part and the real part of a complex number s, respectively. Then, a simple calculation by above lemmas gives

Lemma 8. *For any grid function $u^n \in \mathscr{V}_h$, $0 \le n \le N$, we have*

$$\mathrm{Re}\left(\mathcal{A}_x^\alpha \delta_t u^{n+\frac{1}{2}}, u^{n+\frac{1}{2}} \right) = \frac{1}{2\tau} \left(\|u^{n+1}\|_A^2 - \|u^n\|_A^2 \right), \tag{44}$$

$$\mathrm{Re}\left(\Delta_h^\alpha u^{n+\frac{1}{2}}, \delta_t u^{n+\frac{1}{2}} \right) = \frac{1}{2\tau} \left(\|\Lambda^\alpha u^{n+1}\|^2 - \|\Lambda^\alpha u^n\|^2 \right). \tag{45}$$

Proof. It is obvious that

$$\begin{aligned}\left(\mathcal{A}_x^\alpha \delta_t u^{n+\frac{1}{2}}, u^{n+\frac{1}{2}} \right) &= \frac{1}{2\tau} \left\{ (\mathcal{A}_x^\alpha u^{n+1}, u^{n+1}) + (\mathcal{A}_x^\alpha u^{n+1}, u^n) - (\mathcal{A}_x^\alpha u^n, u^{n+1}) + (\mathcal{A}_x^\alpha u^n, u^n) \right\} \\ &= \frac{1}{2\tau} \left\{ \|u^{n+1}\|_{\mathcal{A}}^2 + (\mathcal{A}_x^\alpha u^{n+1}, u^n) - (\mathcal{A}_x^\alpha u^n, u^{n+1}) + \|u^n\|_{\mathcal{A}}^2 \right\}.\end{aligned}$$

From lemma 5, we have $(\mathcal{A}_x^\alpha u^{n+1}, u^n) = (u^{n+1}, \mathcal{A}_x^\alpha u^n)$. Therefore, we get

$$\mathrm{Re}\left(\mathcal{A}_x^\alpha \delta_t u^{n+\frac{1}{2}}, u^{n+\frac{1}{2}} \right) = \frac{1}{2\tau} \left(\|u^{n+1}\|_A^2 - \|u^n\|_A^2 \right).$$

Similarly as above method and by using lemma 7, we can derive (45). □

Theorem 1. *The quasi-compact difference solution of scheme* (34)–(37) *is conservative in the following senses:*

$$M_1^n \equiv M_1^0, \quad M_2^n \equiv M_2^0, \quad E_1^n \equiv E_1^0, \quad E_2^n \equiv E_2^0, \quad n = 1, 2, \ldots, N, \tag{46}$$

where

$$M_1^n := \|u^n\|_A^2, \qquad M_2^n := \|v^n\|_A^2, \qquad E_1^n := \|\Lambda^\alpha u^n\|^2, \qquad E_2^n := \|\Lambda^\alpha v^n\|^2.$$

Proof. Making the inner product of (34) with $u^{n+\frac{1}{2}}$, taking the imaginary part of the resulting equation, and by using lemma 8, we obtain $M_1^{n+1} = M_1^n$, which implies $M_1^n \equiv M_1^0$ for $n = 1, 2, \ldots, N$. Making the inner product of (34) with $\delta_t u^{n+\frac{1}{2}}$, taking the imaginary part of the resulting equation, and by using lemma 8, we obtain $E_1^{n+1} = E_1^n$, which implies $E_1^n \equiv E_1^0$ for $n = 1, 2, \ldots, N$. Similarly, we can obtain $M_2^n \equiv M_2^0$ and $E_2^n \equiv E_2^0$ for $n = 1, 2, \ldots, N$. □

Remark 1. *Indeed, the mass conservation results (i.e.,* $\|u^n\| \equiv \|u^0\|$ *and* $\|v^n\| \equiv \|v^0\|$, $0 \le n \le N$*) are still valid. We will give the detailed proof in sect.* 5.

Next, we establish the prior boundedness of the discrete solutions.

Theorem 2. *The solutions of the scheme* (34)–(36) *are bounded in the following senses:*

$$\|u^n\| \le C_{u_1}, \quad |u^n|_{H^{\frac{\alpha}{2}}} \le C_{u_2}, \quad \|u^n\|_{l^\infty} \le C_{u_3}, \quad 0 \le n \le N \tag{47}$$

and

$$\|v^n\| \le C_{v_1}, \quad |v^n|_{H^{\frac{\alpha}{2}}} \le C_{v_2}, \quad \|v^n\|_{l^\infty} \le C_{v_3}, \quad 0 \le n \le N, \tag{48}$$

where C_{u_1}, C_{u_2}, C_{u_3}, *and* C_{v_1}, C_{v_2}, C_{v_3} *are some positive constants.*

Proof. From lemma 6 and the compact-norm conservation (46), we easily obtain the first inequality in (47). Then by the conservation result of E_1^n in (46), from lemma 4, the second inequality is arrived at immediately. Finally, combining the first two inequalities in (47) with the discrete Sobolev inequality (18) implies that

$$\|u^n\|_{l^\infty}^2 \le C_\mu^2 \left(\|u^n\|^2 + |u^n|_{H^{\frac{\alpha}{2}}}^2 \right) \le C_\mu^2 (C_{u_1}^2 + C_{u_2}^2) := C_{u_3}^2, \quad 0 \le n \le N.$$

The results of v^n follow analogue. Thus, we complete the proof. □

Finally, we establish the unconditional error estimates of the quasi-compact scheme (34)–(37). For convenience, we define the error functions $e^n \in \mathscr{V}_h$ and $E^n \in \mathscr{V}_h$ as

$$e_j^n = U_j^n - u_j^n, \quad E_j^n = V_j^n - v_j^n, \quad j \in \mathcal{T}_M, \quad 0 \le n \le N.$$

Subtracting (34) from (32), and (35) from (33), we obtain the following error equations:

$$\mathcal{A}_x^\alpha \delta_t e_j^{n+\frac{1}{2}} + i\kappa \Delta_h^\alpha e_j^{n+\frac{1}{2}} = R_j^{n+\frac{1}{2}}, \quad j \in \mathcal{T}_M, \quad 0 \le n \le N-1 \tag{49}$$

and

$$\mathcal{A}_x^\alpha \delta_t E_j^{n+\frac{1}{2}} + i\kappa \Delta_h^\alpha E_j^{n+\frac{1}{2}} = R_j^{n+\frac{1}{2}}, \quad j \in \mathcal{T}_M, \quad 0 \le n \le N-1, \tag{50}$$

with the initial and boundary conditions

$$e_j^0 = 0, \quad j \in \mathcal{T}_M, \tag{51}$$

$$e_j^n = 0, \quad j \in \mathbb{Z} \backslash \mathcal{T}_M, \quad 0 \le n \le N. \tag{52}$$

Theorem 3. *Suppose that the exact solutions of the original problem* (20)–(22) *under the condition* $\rho = 0$ *are sufficiently smooth. Then we have*

$$\|e^n\| + \|E^n\| \le C(\tau^2 + h^4), \quad 0 \le n \le N, \tag{53}$$

where C *is a positive constant independent of* h *and* τ.

Proof. Computing the inner product of (49) with $e^{n+\frac{1}{2}}$, taking the real part of the resulting equation, and by virtue of lemma 8, we obtain

$$\frac{1}{2\tau}(\|e^{n+1}\|_A^2 - \|e^n\|_A^2) = \mathrm{Re}\left(R^{n+\frac{1}{2}}, e^{n+\frac{1}{2}} \right). \tag{54}$$

For the term on the right-hand side of (54), by lemma 6, we have

$$\mathrm{Re}\left(R^{n+\frac{1}{2}}, e^{n+\frac{1}{2}}\right) \le \left\|R^{n+\frac{1}{2}}\right\| \cdot \left\|e^{n+\frac{1}{2}}\right\| \le \left\|R^{n+\frac{1}{2}}\right\| \cdot \sqrt{3}\left\|e^{n+\frac{1}{2}}\right\|_A \le \frac{\sqrt{3}}{2}\left\|R^{n+\frac{1}{2}}\right\| \cdot \left(\|e^{n+1}\|_A + \|e^n\|_A\right). \tag{55}$$

Therefore, from (54) and (55), and by using $\|e^{n+1}\|_A^2 - \|e^n\|_A^2 = (\|e^{n+1}\|_A + \|e^n\|_A)(\|e^{n+1}\|_A - \|e^n\|_A)$, we obtain

$$\|e^{n+1}\|_A \le \|e^n\|_A + \sqrt{3}\tau\left\|R^{n+\frac{1}{2}}\right\|, \tag{56}$$

which further implies

$$\|e^{n+1}\|_A \le \|e^0\|_A + \sqrt{3}\tau\sum_{l=0}^{n}\left\|R^{n+\frac{1}{2}}\right\| \le \sqrt{3}C_R T(\tau^2 + h^4). \tag{57}$$

By lemma 6, we have

$$\|e^{n+1}\| \le \sqrt{3}\|e^{n+1}\|_A \le C(\tau^2 + h^4), \tag{58}$$

where $C = 3C_R T$. Similarly, we can obtain the estimate of $\|E^n\|$. Therefore, we complete the proof of theorem 3. □

5 Conservative properties of the quasi-compact SSFD scheme

In this section, we study the conservative properties of the quasi-compact SSFD scheme (38)–(43). For $u = (u_1, u_2, \cdots, u_{M-1})^T$, we rewrite $\mathcal{A}_x^\alpha u$ and $\Delta_h^\alpha u$ in the matrix forms

$$\mathcal{A}_x^\alpha u = Au, \qquad \Delta_h^\alpha u = \frac{1}{h^\alpha}Cu, \tag{59}$$

where matrix A is a symmetric tri-diagonal matrix of $(M-1)$-square, and matrix $C := \frac{1}{2\cos\frac{\alpha\pi}{2}}(\mathbf{W}^{(\alpha)} + (\mathbf{W}^{(\alpha)})^T) \in \mathbb{R}^{(M-1)\times(M-1)}$,

$$\mathbf{W}^{(\alpha)} = \begin{pmatrix} w_1^{(\alpha)} & w_0^{(\alpha)} & & & \\ w_2^{(\alpha)} & w_1^{(\alpha)} & w_0^{(\alpha)} & & \\ \vdots & w_2^{(\alpha)} & w_1^{(\alpha)} & \ddots & \\ w_{M-2}^{(\alpha)} & \vdots & \ddots & \ddots & w_0^{(\alpha)} \\ w_{M-1}^{(\alpha)} & w_{M-2}^{(\alpha)} & \cdots & w_2^{(\alpha)} & w_1^{(\alpha)} \end{pmatrix} \in \mathbb{R}^{(M-1)\times(M-1)}.$$

From [19,60,64], we know that A and C are real-valued symmetric positive-definite matrices.

After above preparations, we now turn to prove the conservation properties of the quasi-compact SSFD scheme.

Theorem 4. *The quasi-compact SSFD method* (34)–(36) *is conservative in the senses*

$$M_u^n \equiv M_u^0, \quad M_v^n \equiv M_v^0, \quad 0 \le n \le N, \tag{60}$$

where

$$M_u^n := \|u^n\|^2, \qquad M_v^n := \|v^n\|^2,$$

are the mass in the discrete senses.

Proof. Denote $u = \varphi + i\psi$ and $\tilde{u} = (\varphi_1, \varphi_2, \cdots, \varphi_{M-1}, \psi_1, \psi_2, \cdots, \psi_{M-1})^T$. It follows from (40) and (59) that

$$H\tilde{u}^{n(2)} = H^T\tilde{u}^{n(1)}, \tag{61}$$

where

$$H := \begin{pmatrix} A & -rC \\ rC & A \end{pmatrix}, \quad r := \frac{\kappa\tau}{2h^\alpha}.$$

It is obvious that

$$HH^T = H^TH = \begin{pmatrix} A^2 + r^2C^2 & \mathbf{0} \\ \mathbf{0} & A^2 + r^2C^2 \end{pmatrix}. \tag{62}$$

Hence, we have

$$(HH^T)^{-1}(H^TH) = (HH^T)^{-1}(HH^T) = I.$$

Then, we obtain

$$H(HH^T)^{-1}H^T = I.$$

Therefore, we conclude that

$$\|H^{-1}H^T\| = \sqrt{\rho([H^{-1}H^T]^T[H^{-1}H^T])} = \sqrt{\rho(H(HH^T)^{-1}H^T)} = 1. \tag{63}$$

It follows from (62) and (63) that

$$\|\tilde{u}^{n(2)}\| = \|H^{-1}H^T\tilde{u}^{n(1)}\| \le \|H^{-1}H^T\| \cdot \|\tilde{u}^{n(1)}\| \le \|\tilde{u}^{n(1)}\|. \tag{64}$$

Similarly, we have

$$\|\tilde{u}^{n(1)}\| \le \|\tilde{u}^{n(2)}\|. \tag{65}$$

Therefore, by using (64) and (65), we get

$$\|\tilde{u}^{n(2)}\| = \|\tilde{u}^{n(1)}\|. \tag{66}$$

Thus, it follows from (66) that

$$\|u^{n(2)}\| = \|u^{n(1)}\|. \tag{67}$$

Further, according to (38) and (42), we get

$$\|u^n\| = \|u^{n(1)}\|, \qquad \|u^{n(2)}\| = \|u^{n+1}\|. \tag{68}$$

Consequently, combining (67) with (68) implies $M_u^n \equiv M_u^0$. Similarly, we can conclude $M_v^n \equiv M_v^0$. Therefore, the proof is completed. □

Remark 2. *The compact split-step difference scheme and the corresponding conclusions can be expended to K-coupled Schrödinger equations*

$$iu_{lt} - \kappa(-\Delta)^{\frac{\alpha}{2}}u_l + \left(\sum_{s=1}^{K}\rho_{ls}|u_s|^2\right)u_l = 0, \quad x \in \mathbb{R},\ t > 0,\ l = 0, 1\cdots, K. \tag{69}$$

We will show some numerical examples to illustrate some properties of (69) *instead of stating them here for brevity of the paper.*

6 Extension to the two-dimensional problem

In this section, we adopt the quasi-compact SSFD method to solve the two-dimensional space fractional CNLS

$$iu_t - \kappa\left[(-\Delta_x)^{\frac{\alpha}{2}}u + (-\Delta_y)^{\frac{\alpha}{2}}u\right] + \rho(|u|^2 + \beta|v|^2)u = 0, \quad (x, y, t) \in \Omega^d \times (0, T], \tag{70}$$

$$iv_t - \kappa\left[(-\Delta_x)^{\frac{\alpha}{2}}v + (-\Delta_y)^{\frac{\alpha}{2}}v\right] + \rho(|v|^2 + \beta|u|^2)v = 0, \quad (x, y, t) \in \Omega^d \times (0, T], \tag{71}$$

$$u(x, y, 0) = u_0(x, y), \quad v(x, y, 0) = v_0(x, y), \quad (x, y) \in \Omega^d, \tag{72}$$

$$u(x, y, t) = 0, \quad (x, y, t) \in \partial\Omega^d \times (0, T], \tag{73}$$

where $\Omega^d = \Omega_x^d \times \Omega_y^d = (a, b) \times (c, d)$.

We denote $h_x = (b - a)/M_1$ and $h_y = (d - c)/M_2$. Define a partition of $[a, b] \times [c, d]$ by $\Omega_{h_x}^d \times \Omega_{h_y}^d$ with the grid $\Omega_{h_x}^d = \{x_j = a + jh_x;\ j = 0, 1, \cdots, M_1\}$ and $\Omega_{h_y}^d = \{y_j = c + jh_y;\ j = 0, 1, \cdots, M_2\}$. In addition, we denote the index set $\mathcal{T}_{M_1\times M_2} = \{(i, j) \mid i = 1, 2, \cdots, M_1 - 1, j = 1, 2, \cdots, M_2 - 1\}$. Similarly as the one-dimensional case, we define

$$\Delta_h^\alpha u(x, y, t) = \Delta_{h_x}^\alpha u(x, y, t) + \Delta_{h_y}^\alpha u(x, y, t),$$

where $\Delta_{h_x}^\alpha u(x, y, t)$ and $\Delta_{h_y}^\alpha u(x, y, t)$ are given by (25) in the x- and y-direction, respectively, in which, ${}_L\mathscr{D}_{h_x}^\alpha u(x, y, t)$ (or ${}_L\mathscr{D}_{h_y}^\alpha u(x, y, t)$) and ${}_R\mathscr{D}_{h_x}^\alpha u(x, y, t)$ (or ${}_R\mathscr{D}_{h_y}^\alpha u(x, y, t)$) are denoted by (24). Then, denote $\mathcal{A}_x^\alpha$ and $\mathcal{A}_y^\alpha$ be the quasi-compact operators in the x- and y-direction, respectively. Similarly as the one-dimensional case, one obtains

$$\Delta_{h_x}^\alpha u(x, y, t) = \mathcal{A}_x^\alpha((-\Delta_x)^{\frac{\alpha}{2}}u(x, y, t)) + O(h_x^4), \qquad \Delta_{h_y}^\alpha u(x, y, t) = \mathcal{A}_y^\alpha((-\Delta_y)^{\frac{\alpha}{2}}u(x, y, t)) + O(h_y^4). \tag{74}$$

In what follows, we first consider the linear space fractional CNLS, *i.e.*, $\rho = 0$. A simple calculation yields

$$\mathcal{A}_x^\alpha \mathcal{A}_y^\alpha \delta_t U_{i,j}^{n+\frac{1}{2}} + i\kappa \left[\mathcal{A}_y^\alpha \Delta_{h_x}^\alpha U_{i,j}^{n+\frac{1}{2}} + \mathcal{A}_x^\alpha \Delta_{h_y}^\alpha U_{i,j}^{n+\frac{1}{2}}\right] = R_U^{n+\frac{1}{2}}, \quad (i,j) \in \mathcal{T}_{M_1\times M_2},\ 1 \le n \le N-1, \tag{75}$$

$$\mathcal{A}_x^\alpha \mathcal{A}_y^\alpha \delta_t V_{i,j}^{n+\frac{1}{2}} + i\kappa \left[\mathcal{A}_y^\alpha \Delta_{h_x}^\alpha V_{i,j}^{n+\frac{1}{2}} + \mathcal{A}_x^\alpha \Delta_{h_y}^\alpha V_{i,j}^{n+\frac{1}{2}}\right] = R_V^{n+\frac{1}{2}}, \quad (i,j) \in \mathcal{T}_{M_1\times M_2},\ 1 \le n \le N-1, \tag{76}$$

where $R_U^{n+\frac{1}{2}}$ and $R_V^{n+\frac{1}{2}}$ denote the truncation errors. Obviously, we have

$$\left|R_U^{n+\frac{1}{2}}\right| \le C_{R_U}(\tau^2 + h_x^4 + h_y^4),$$

$$\left|R_V^{n+\frac{1}{2}}\right| \le C_{R_V}(\tau^2 + h_x^4 + h_y^4),$$

where C_{R_U} and C_{R_V} are positive constants independent of h and τ. Adding the small items $-\frac{\tau^2}{4}\Delta_{h_x}^\alpha \Delta_{h_y}^\alpha \delta_t U_{i,j}^{n+\frac{1}{2}}$ and $-\frac{\tau^2}{4}\Delta_{h_x}^\alpha \Delta_{h_y}^\alpha \delta_t V_{i,j}^{n+\frac{1}{2}}$ into (75) and (76) respectively, one obtains

$$\left(\mathcal{A}_x^\alpha + i\frac{\tau}{2}\Delta_{h_x}^\alpha\right)\left(\mathcal{A}_y^\alpha + i\frac{\tau}{2}\Delta_{h_y}^\alpha\right) U_{i,j}^{n+1} = \left(\mathcal{A}_x^\alpha - i\frac{\tau}{2}\Delta_{h_x}^\alpha\right)\left(\mathcal{A}_y^\alpha - i\frac{\tau}{2}\Delta_{h_y}^\alpha\right) U_{i,j}^{n+1} + \hat{R}_U^{n+\frac{1}{2}}, \tag{77}$$

$$\left(\mathcal{A}_x^\alpha + i\frac{\tau}{2}\Delta_{h_x}^\alpha\right)\left(\mathcal{A}_y^\alpha + i\frac{\tau}{2}\Delta_{h_y}^\alpha\right) V_{i,j}^{n+1} = \left(\mathcal{A}_x^\alpha - i\frac{\tau}{2}\Delta_{h_x}^\alpha\right)\left(\mathcal{A}_y^\alpha - i\frac{\tau}{2}\Delta_{h_y}^\alpha\right) V_{i,j}^{n+1} + \hat{R}_V^{n+\frac{1}{2}}, \tag{78}$$

where

$$\hat{R}_U^{n+\frac{1}{2}} = R_U^{n+\frac{1}{2}} - \frac{\tau^2}{4}\Delta_{h_x}^\alpha \Delta_{h_y}^\alpha \delta_t U_{i,j}^{n+\frac{1}{2}},$$

$$\hat{R}_V^{n+\frac{1}{2}} = R_V^{n+\frac{1}{2}} - \frac{\tau^2}{4}\Delta_{h_x}^\alpha \Delta_{h_y}^\alpha \delta_t V_{i,j}^{n+\frac{1}{2}}.$$

It is obvious that

$$\left|\hat{R}_U^{n+\frac{1}{2}}\right| = O(\tau^2 + h_x^4 + h_y^4),$$

$$\left|\hat{R}_V^{n+\frac{1}{2}}\right| = O(\tau^2 + h_x^4 + h_y^4).$$

Then, removing the local truncation errors $\hat{R}_U^{n+\frac{1}{2}}$ and $\hat{R}_V^{n+\frac{1}{2}}$ in (77)–(78) arrives at the following alternating direction implicit (ADI) difference schemes

$$\left(\mathcal{A}_x^\alpha + i\frac{\tau}{2}\Delta_{h_x}^\alpha\right)\left(\mathcal{A}_y^\alpha + i\frac{\tau}{2}\Delta_{h_y}^\alpha\right) u_{i,j}^{n+1} = \left(\mathcal{A}_x^\alpha - i\frac{\tau}{2}\Delta_{h_x}^\alpha\right)\left(\mathcal{A}_y^\alpha - i\frac{\tau}{2}\Delta_{h_y}^\alpha\right) u_{i,j}^{n}, \tag{79}$$

$$\left(\mathcal{A}_x^\alpha + i\frac{\tau}{2}\Delta_{h_x}^\alpha\right)\left(\mathcal{A}_y^\alpha + i\frac{\tau}{2}\Delta_{h_y}^\alpha\right) v_{i,j}^{n+1} = \left(\mathcal{A}_x^\alpha - i\frac{\tau}{2}\Delta_{h_x}^\alpha\right)\left(\mathcal{A}_y^\alpha - i\frac{\tau}{2}\Delta_{h_y}^\alpha\right) v_{i,j}^{n}, \tag{80}$$

$$u_{i,j}^0 = u_0(x_i, y_j), \quad v_{i,j}^0 = v_0(x_i, y_j), \quad (i,j) \in \mathbb{Z}^2, \tag{81}$$

$$u_{i,j}^n = 0, \quad v_{i,j}^n = 0, \quad (i,j) \in \mathbb{Z}^2 \backslash \mathcal{T}_{M_1\times M_2}, \quad 1 \le n \le N. \tag{82}$$

To seek the solutions u^{n+1} and v^{n+1}, the Peaceman-Rachford ADI scheme is adopted. Firstly, we solve

$$\left(\mathcal{A}_x^\alpha + i\frac{\tau}{2}\Delta_{h_x}^\alpha\right) u_{i,j}^* = \left(\mathcal{A}_y^\alpha - i\frac{\tau}{2}\Delta_{h_y}^\alpha\right) u_{i,j}^n, \qquad \left(\mathcal{A}_x^\alpha + i\frac{\tau}{2}\Delta_{h_x}^\alpha\right) v_{i,j}^* = \left(\mathcal{A}_y^\alpha - i\frac{\tau}{2}\Delta_{h_y}^\alpha\right) v_{i,j}^n, \tag{83}$$

and then

$$\left(\mathcal{A}_y^\alpha + i\frac{\tau}{2}\Delta_{h_y}^\alpha\right) u_{i,j}^{n+1} = \left(\mathcal{A}_x^\alpha - i\frac{\tau}{2}\Delta_{h_x}^\alpha\right) u_{i,j}^*, \qquad \left(\mathcal{A}_y^\alpha + i\frac{\tau}{2}\Delta_{h_y}^\alpha\right) v_{i,j}^{n+1} = \left(\mathcal{A}_x^\alpha - i\frac{\tau}{2}\Delta_{h_x}^\alpha\right) v_{i,j}^*, \tag{84}$$

where $(i,j) \in \mathcal{T}_{M_1\times M_2}$, $1 \le n \le N-1$. Denote $e_{i,j}^n = U_{i,j}^n - u_{i,j}^n$ and $E_{i,j}^n = V_{i,j}^n - v_{i,j}^n$, $0 \le n \le N$. Then, one obtains the error equations

$$\left(\mathcal{A}_x^\alpha + i\frac{\tau}{2}\Delta_{h_x}^\alpha\right)\left(\mathcal{A}_y^\alpha + i\frac{\tau}{2}\Delta_{h_y}^\alpha\right) e_{i,j}^{n+1} = \left(\mathcal{A}_x^\alpha - i\frac{\tau}{2}\Delta_{h_x}^\alpha\right)\left(\mathcal{A}_y^\alpha - i\frac{\tau}{2}\Delta_{h_y}^\alpha\right) e_{i,j}^{n} + \hat{R}_U^{n+\frac{1}{2}}, \tag{85}$$

$$\left(\mathcal{A}_x^\alpha + i\frac{\tau}{2}\Delta_{h_x}^\alpha\right)\left(\mathcal{A}_y^\alpha + i\frac{\tau}{2}\Delta_{h_y}^\alpha\right) E_{i,j}^{n+1} = \left(\mathcal{A}_x^\alpha - i\frac{\tau}{2}\Delta_{h_x}^\alpha\right)\left(\mathcal{A}_y^\alpha - i\frac{\tau}{2}\Delta_{h_y}^\alpha\right) E_{i,j}^{n} + \hat{R}_V^{n+\frac{1}{2}}. \tag{86}$$

Then, similarly as theorem 3.3 in [26], we arrive at the following approximation results.

Theorem 5. *Suppose that the exact solutions of the original problem* (70)–(73) *under the condition* $\rho = 0$ *are sufficiently smooth. Then we have for* $0 \le n \le N$,

$$\|e^n\| \le C_e(\tau^2 + h_x^4 + h_y^4), \qquad \|E^n\| \le C_E(\tau^2 + h_x^4 + h_y^4), \tag{87}$$

where C_e *and* C_E *are positive constants independent of* h_x, h_y *and* τ.

For the nonlinear system (70)–(73), we put forward a split-step algorithm as follows.

Algorithms. The quasi-compact ADI SSFD method for the nonlinear two-dimensional space fractional CNLS (70)–(73) from time t_n to time t_{n+1}, $1 \le n \le N-1$.

Step 1: for $i = 0(1)M_1$, $j = 0(1)M_2$

$$u_{i,j}^{n(1)} = \exp\left\{i\rho\left(|u_{i,j}^n|^2 + \beta|v_{i,j}^n|^2\right)\tau/2\right\} u_{i,j}^n, \tag{88}$$

$$v_{i,j}^{n(1)} = \exp\left\{i\rho\left(|v_{i,j}^n|^2 + \beta|u_{i,j}^n|^2\right)\tau/2\right\} v_{i,j}^n. \tag{89}$$

Step 2: for $i = 1(1)M_1 - 1$, $j = 1(1)M_2 - 1$

$$\left(\mathcal{A}_x^\alpha + i\frac{\tau}{2}\Delta_{h_x}^\alpha\right)\left(\mathcal{A}_y^\alpha + i\frac{\tau}{2}\Delta_{h_y}^\alpha\right) u_{i,j}^{n(2)} = \left(\mathcal{A}_x^\alpha - i\frac{\tau}{2}\Delta_{h_x}^\alpha\right)\left(\mathcal{A}_y^\alpha - i\frac{\tau}{2}\Delta_{h_y}^\alpha\right) u_{i,j}^{n(1)}, \tag{90}$$

$$\left(\mathcal{A}_x^\alpha + i\frac{\tau}{2}\Delta_{h_x}^\alpha\right)\left(\mathcal{A}_y^\alpha + i\frac{\tau}{2}\Delta_{h_y}^\alpha\right) v_{i,j}^{n(2)} = \left(\mathcal{A}_x^\alpha - i\frac{\tau}{2}\Delta_{h_x}^\alpha\right)\left(\mathcal{A}_y^\alpha - i\frac{\tau}{2}\Delta_{h_y}^\alpha\right) v_{i,j}^{n(1)}. \tag{91}$$

Step 3: for $i = 0(1)M_1$, $j = 0(1)M_2$

$$u_{i,j}^{n+1} = \exp\left\{i\rho\left(\left|u_{i,j}^{n(2)}\right|^2 + \beta\left|v_{i,j}^{n(2)}\right|^2\right)\tau/2\right\} u_{i,j}^{n(2)}, \tag{92}$$

$$v_{i,j}^{n+1} = \exp\left\{i\rho\left(\left|v_{i,j}^{n(2)}\right|^2 + \beta\left|u_{i,j}^{n(2)}\right|^2\right)\tau/2\right\} v_{i,j}^{n(2)}. \tag{93}$$

For the difference scheme (88)–(93), the mass conservation results can be obtained following similar lines as theorem 4. For brevity of the paper, we omit the proof here.

7 Numerical experiments

All our tests are performed under MATLAB 2012a on a Dell desktop with i7-4790 CPU and 8 GB memory.

Example 1. *Consider* (1)–(3) *with the initial conditions* [20–22, 45, 46]

$$u(x,0) = \operatorname{sech}(x + D_0)\cdot\exp(iV_0x),$$
$$v(x,0) = \operatorname{sech}(x - D_0)\cdot\exp(-iV_0x). \tag{94}$$

In this example, the considered domain is $(x,t) \in [-20,20]\times[0,T]$, *and we choose the parameters* $D_0 = 10$, $V_0 = 3$, $\kappa = 1$, $\rho = 1$ *and* $\beta = 3$.

Firstly, the convergent rates in temporal and spatial directions for the quasi-compact SSFD method are checked. We obtain the numerical "exact" solutions U^n and V^n by the schemes with a very fine mesh and a small time step, *e.g.* $h = 0.0125$ and $\tau = 0.0001$. In order to check the temporal convergent rate, the spatial step is fixed small enough. Moreover, to check the spatial convergent rate, we take the temporal step sufficiently small. In this example, we choose $h = 0.0125$ and $\tau = 0.0001$, respectively. Due to the consistency of the errors and convergence orders for u^n and v^n, we only plot the errors between the numerical solution u^n and the "exact" solution U^n in fig. 1 which show that the scheme is of second order in temporal direction and fourth order in spatial direction. In this experiment, we take $T = 1$ and denote $e_u = u^n - U^n$.

Secondly, we study the conservation laws in the mass sense. Define $Q_u^n = \|u^n\|$ and $Q_v^n = \|v^n\|$ for $0 \le n \le N$. Table 1 and fig. 2 show the values of $|\frac{Q_u^n - Q_u^0}{Q_u^0}|$ or $|\frac{Q_v^n - Q_v^0}{Q_v^0}|$ for different values of α. We observe that the scheme is conservative in the mass, and this supports the result of theorem 4. In this experiment, we choose $\tau = h = 0.05$.

Finally, we compare the errors via the SSFD method and quasi-compact SSFD method which show that although the CPU time of both methods are almost the same, the quasi-compact SSFD method is more accurate than the SSFD method (see table 2).

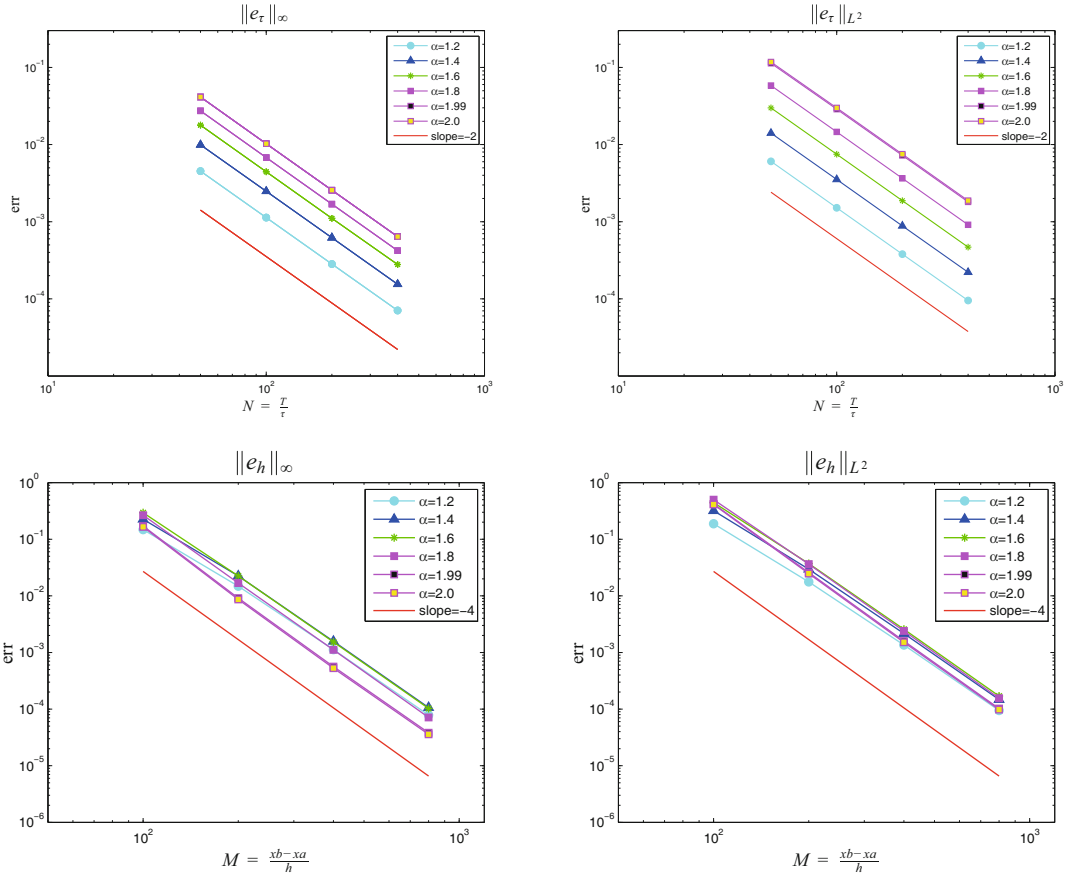

Fig. 1. Convergent rate in time and space.

Table 1. The values of $|\frac{Q_u^n - Q_u^0}{Q_u^0}|$ or $|\frac{Q_v^n - Q_v^0}{Q_v^0}|$ for different α and $\tau = h = 0.05$.

α	$t = 1$	$t = 3$	$t = 5$
1.2	2.8060e-12	2.6917e-10	3.6133e-10
1.5	4.4795e-12	4.2922e-12	2.7960e-10
1.8	1.7175e-12	1.4351e-12	6.3387e-11
2.0	4.7103e-16	4.7103e-16	5.1813e-15

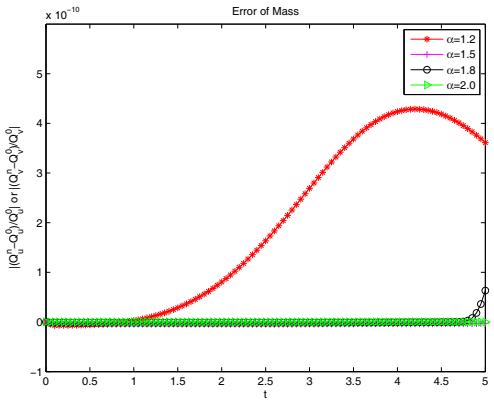

Fig. 2. The conservation laws of Q_u^n and Q_v^n.

Table 2. Comparison of errors via SSFD and compact SSFD for different α.

α	SSFD		Compact SSFD	
	L^∞-error	L^2-error	L^∞-error	L^2-error
1.2	1.1580e-01	1.6164e-01	2.2492e-03	2.8173e-03
1.4	1.3449e-01	1.9423e-01	4.0584e-03	5.6457e-03
1.6	1.2795e-01	2.1656e-01	5.9709e-03	1.0051e-02
1.8	1.0717e-01	2.2449e-01	7.8972e-03	1.7008e-02
2.0	8.7339e-02	2.2764e-01	1.1061e-02	3.1426e-02

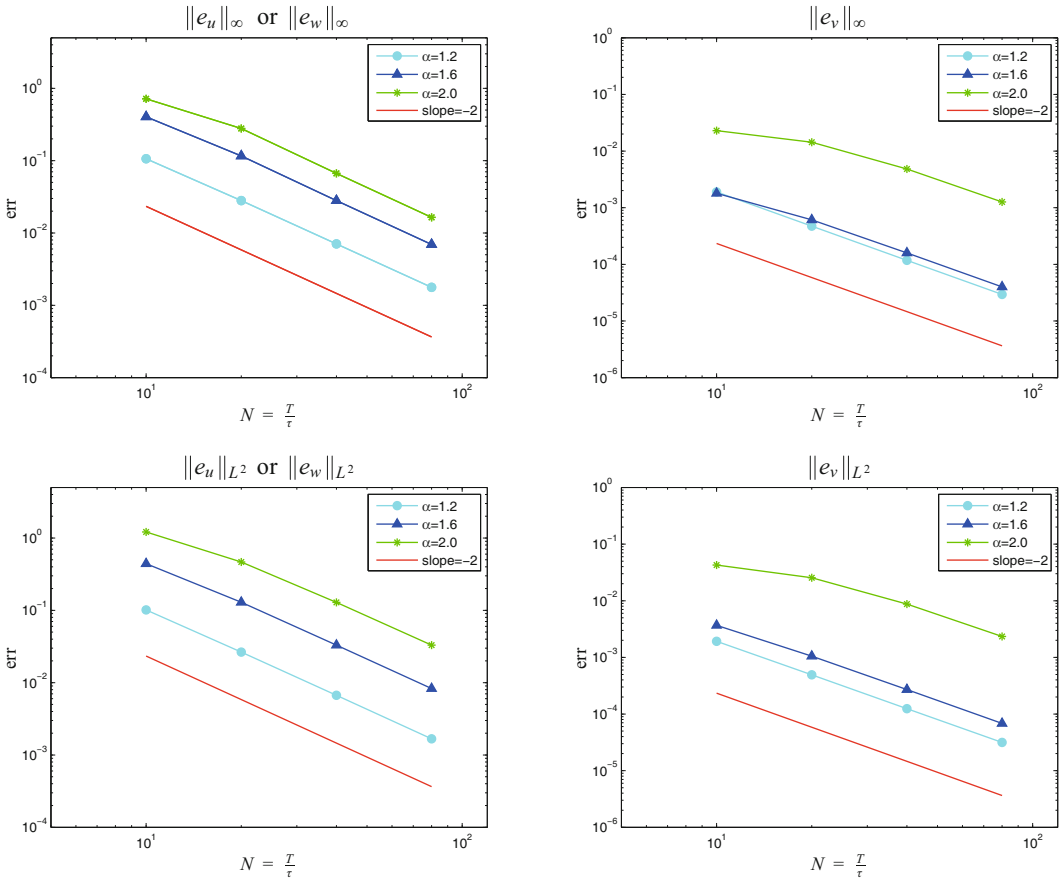

Fig. 3. Convergent rates of u, v and w in temporal direction.

Example 2. *In this example, we consider the following 3-coupled fractional Schrödinger equations* [20–22,45,46]

$$iu_t - \kappa(-\Delta)^{\frac{\alpha}{2}}u + \rho(|u|^2 + \beta|v|^2 + \beta|w|^2)u = 0, \quad x \in \Omega,\ t > 0, \tag{95}$$

$$iv_t - \kappa(-\Delta)^{\frac{\alpha}{2}}v + \rho(|v|^2 + \beta|u|^2 + \beta|w|^2)v = 0, \quad x \in \Omega,\ t > 0, \tag{96}$$

$$iw_t - \kappa(-\Delta)^{\frac{\alpha}{2}}w + \rho(|w|^2 + \beta|u|^2 + \beta|v|^2)w = 0, \quad x \in \Omega,\ t > 0, \tag{97}$$

where the initial conditions are given by

$$u(x,0) = \mathrm{sech}(x + D_0)\cdot\exp(iV_0x), \qquad v(x,0) = \mathrm{sech}(x), \qquad w(x,0) = \mathrm{sech}(x - D_0)\cdot\exp(-iV_0x). \tag{98}$$

In this example, we choose the considered domain $(x,t) \in [-20,20]\times[0,T]$.

Firstly, similar as example 1, in order to check the convergence order of the difference scheme, we firstly obtain the numerical "exact" solutions U^n, V^n and W^n by the schemes with a very fine mesh and a small time step, *e.g.* $h = 0.025$ and $\tau = 0.0001$. To check the convergence order of τ and h, we plot the errors of u^n (w^n) and v^n in fig. 3 and fig. 4. In this experiment, we choose the parameters $D_0 = 10$, $V_0 = 3$, $\kappa = 1$, $\rho = 1$ and $\beta = 3$.

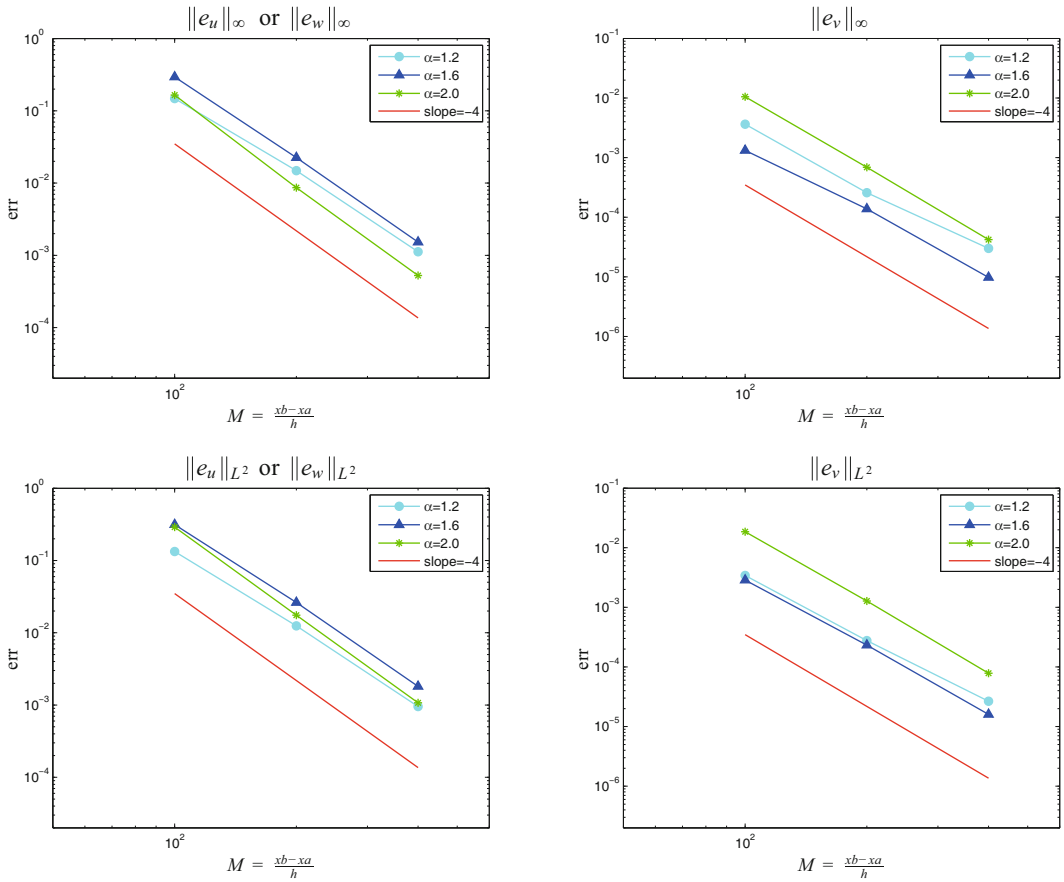

Fig. 4. Convergent rates of u, v and w in spatial direction.

Table 3. The values of $|\frac{Q_u^n - Q_u^0}{Q_u^0}|$ or $|\frac{Q_w^n - Q_w^0}{Q_w^0}|$ for different α and $\tau = h = 0.05$.

α	$t = 1$	$t = 3$	$t = 5$
1.2	2.7927e-12	2.6178e-10	1.8549e-10
1.4	4.5096e-12	4.9189e-12	4.3988e-12
1.6	3.7188e-12	3.7150e-12	3.4675e-12
2.0	1.7271e-15	2.0411e-15	2.8262e-15

Table 4. The values of $|\frac{Q_v^n - Q_v^0}{Q_v^0}|$ for different α and $\tau = h = 0.05$.

α	$t = 1$	$t = 3$	$t = 5$
1.2	8.9679e-10	3.6956e-09	4.3082e-09
1.4	1.7854e-10	6.9538e-10	5.1844e-10
1.6	2.8206e-11	7.9693e-11	5.9786e-11
2.0	1.9940e-14	5.2912e-14	8.8239e-14

Secondly, we study the conservation laws in the mass sense. See the details in table 3, table 4 and fig. 5.

Finally, we check that the order α will affect the shape of the soliton. From figs. 6–8, it is observed that the order α dramatically influences the collision points of the three waves. In this experiment, we choose the parameters $D_0 = 10$, $V_0 = 3$, $\kappa = 1/2$, $\rho = 1$ and $\beta = 2$.

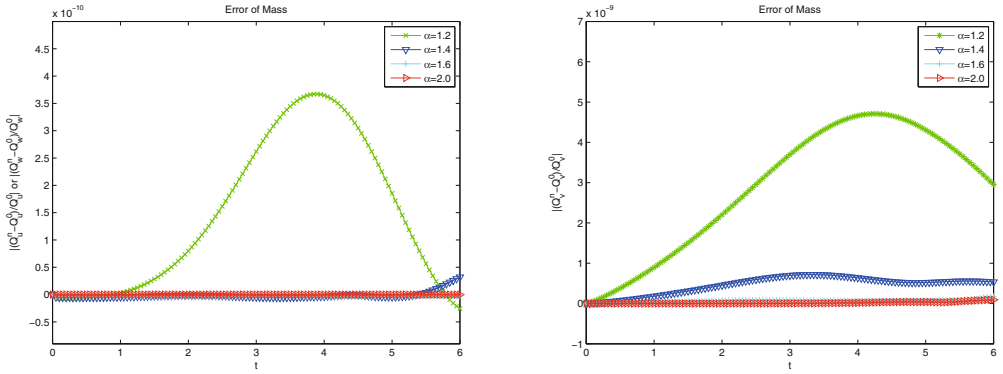

Fig. 5. The conservation laws of Q_u^n, Q_v^n and Q_w^n.

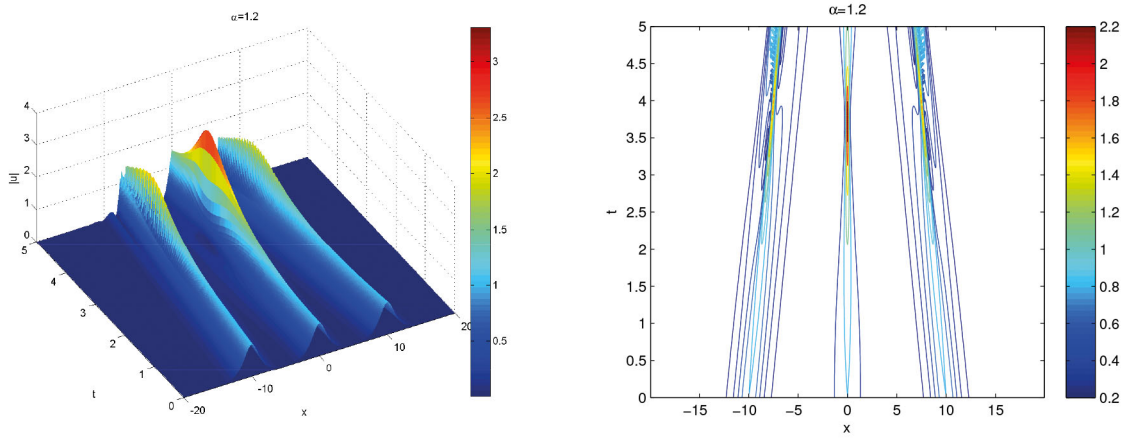

Fig. 6. Profile (left) and contour plot (right) of $|u|$, $|v|$ and $|w|$ for $\alpha = 1.2$.

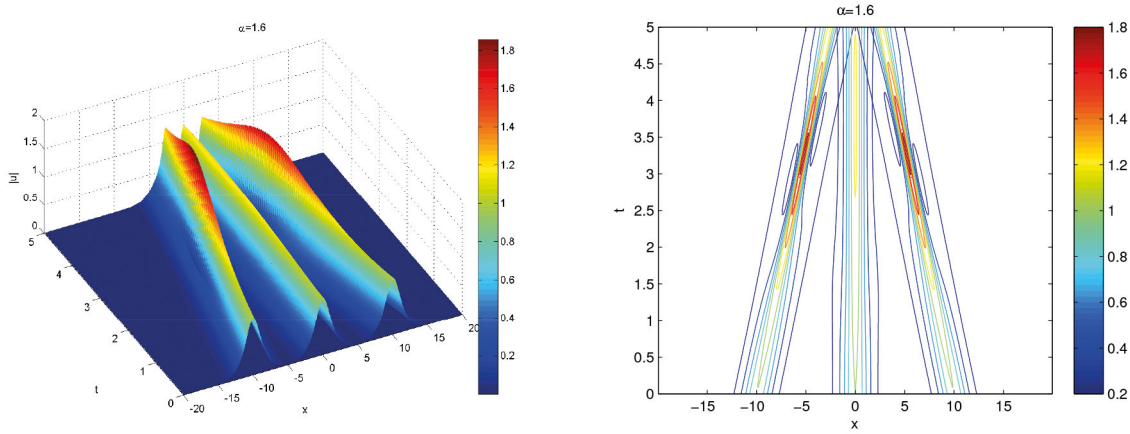

Fig. 7. Profile (left) and contour plot (right) of $|u|$, $|v|$ and $|w|$ for $\alpha = 1.6$.

Example 3. *Consider* (70)–(73) *with the initial conditions* [26, 45, 46]

$$u(x,y,0) = \frac{2}{\sqrt{\pi}} \exp\left(-[(x-3)^2 + (y-3)^2]\right), \qquad v(x,y,0) = \frac{2}{\sqrt{\pi}} \exp\left(-[(x+3)^2 + (y+3)^2]\right). \tag{99}$$

In this example, the considered domain is $(x,y,t) \in [-10,10] \times [-10,10] \times [0,T]$, *and we choose the parameters* $\kappa = 1$, $\rho = 1$ *and* $\beta = 3$.

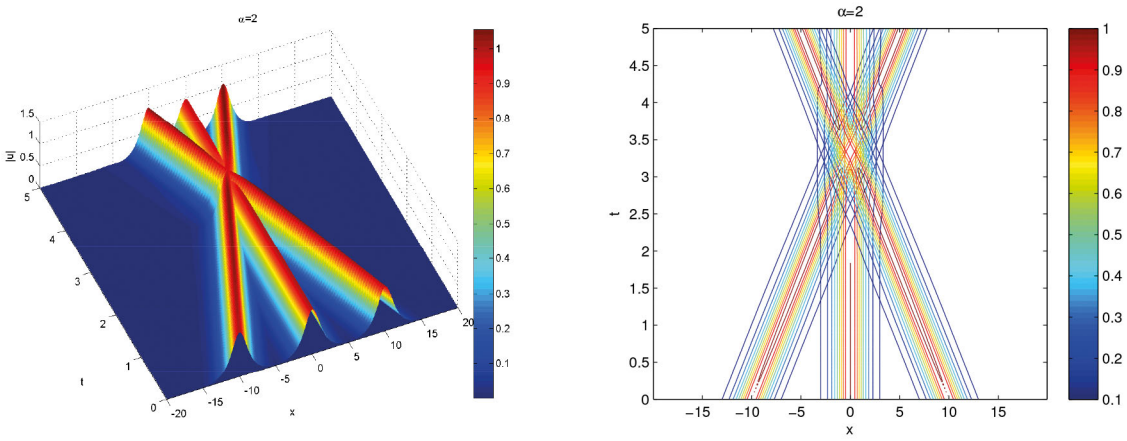

Fig. 8. Profile (left) and contour plot (right) of $|u|$, $|v|$ and $|w|$ for $\alpha = 2.0$.

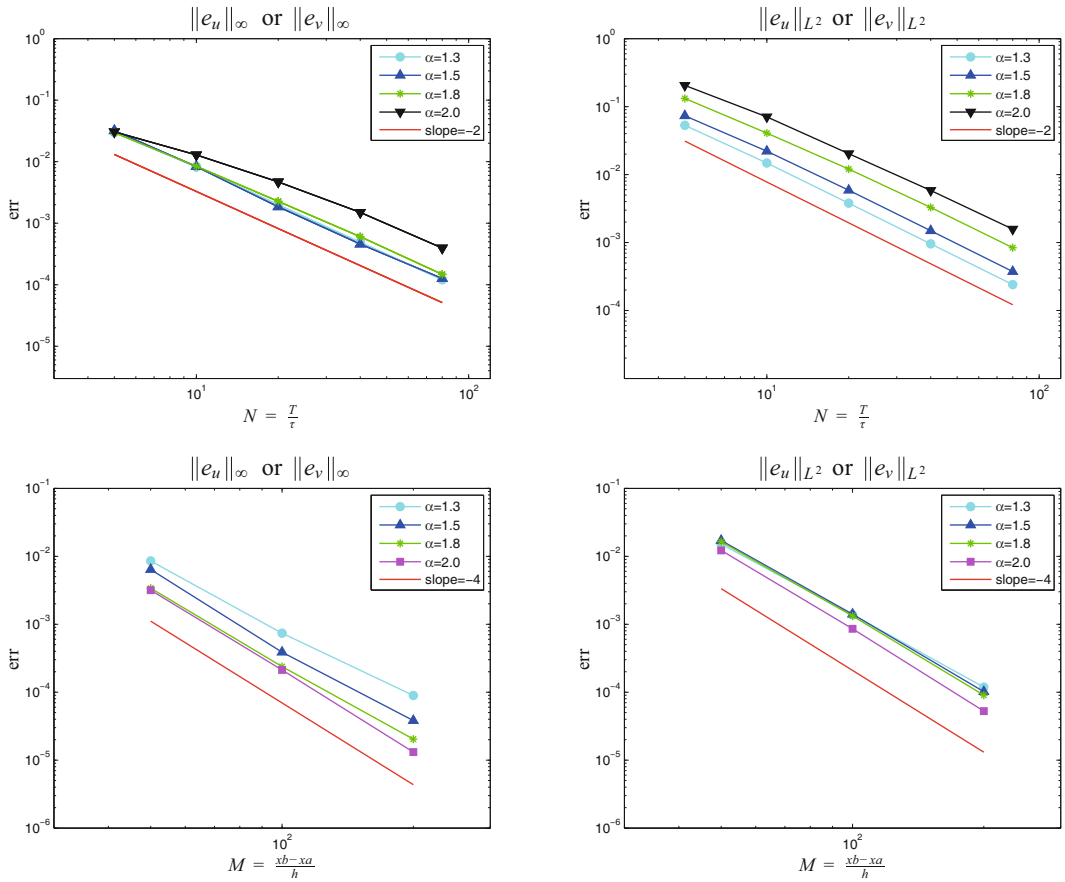

Fig. 9. Convergent rates of u and v in time and space.

Firstly, the convergence orders of the quasi-compact ADI SSFD method in time and space are given in fig. 9, respectively. The numerical "exact" solutions U^n and V^n by the schemes with a very fine mesh and a small time step, *e.g.* $h = 0.025$ and $\tau = 0.0001$. It follows that the convergence order is $O(\tau^2 + h^4)$.

Secondly, by comparing the CPU times with the QCCN scheme, QCIM scheme, QCLI scheme and QCLII scheme, we show the dramatic efficiency of the high-order quasi-compact split-step ADI (QCSSADI) scheme. We propose the schemes in the appendix and the results of the comparison are given in table 5.

Table 5. The CPU times of the CCN scheme, CIM scheme, CLI scheme and CLII scheme (seconds).

α	M	QCCN	QCIM	QCLI	QCLII	QCSSADI
1.2	25	1.6468	1.4127	7.9939	1.8103	0.0646
	50	37.5997	35.3218	333.1728	43.8226	0.1098
1.5	25	1.4375	1.4759	7.8439	1.8210	0.0429
	50	33.1416	35.3218	333.1728	43.8226	0.1079
1.8	25	1.3895	1.3662	8.2093	1.7239	0.0418
	50	31.4152	31.7364	313.1218	42.2711	0.0956
2.0	25	1.3622	1.3224	8.2345	1.7581	0.0420
	50	32.2549	31.3459	330.1181	41.1651	0.1188

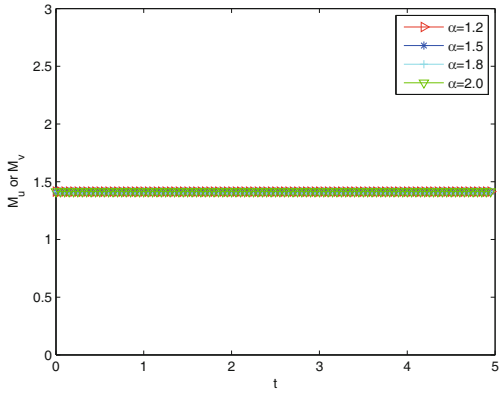

Fig. 10. The conservation laws of Q_u^n and Q_v^n.

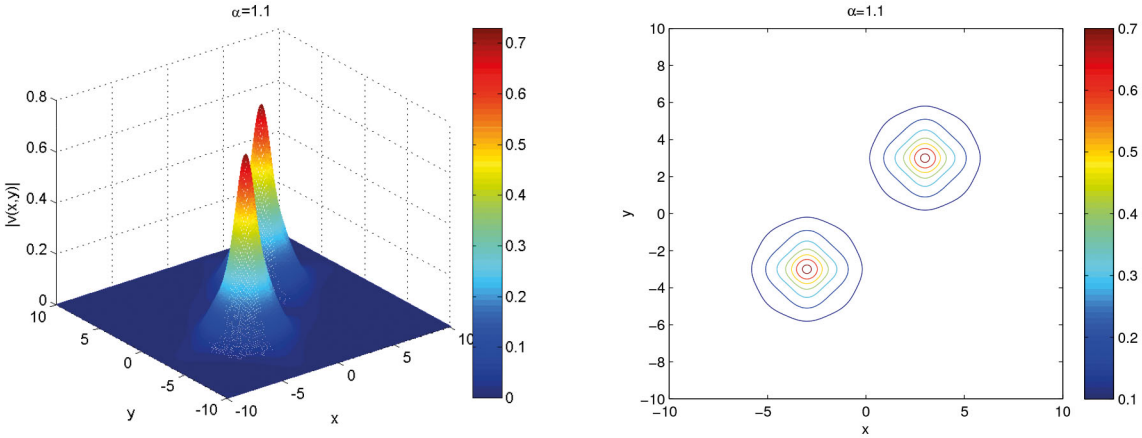

Fig. 11. Profile (left) and contour plot (right) of $|u|$ and $|v|$ for $\alpha = 1.1$.

Then, we also examine the conservation property of the QCSSADI scheme. The conservation results are shown in fig. 10.

Finally, we use the QCSSADI scheme to simulate the dynamics of the model. Figures 11–14 depict the profiles and contours of the wave functions with different α. It follows that the order α will affect the shape of the soliton. We observe that as the decrease of α, the wave functions decay significantly faster, and moreover, the wave shapes becoming taller and steeper. We get similar conclusions as the one-wave cases [26].

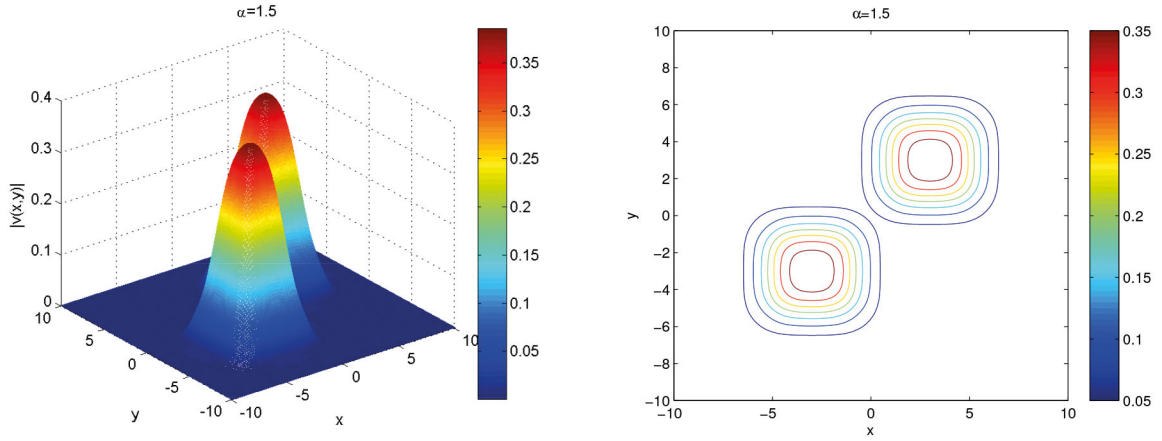

Fig. 12. Profile (left) and contour plot (right) of $|u|$ and $|v|$ for $\alpha = 1.5$.

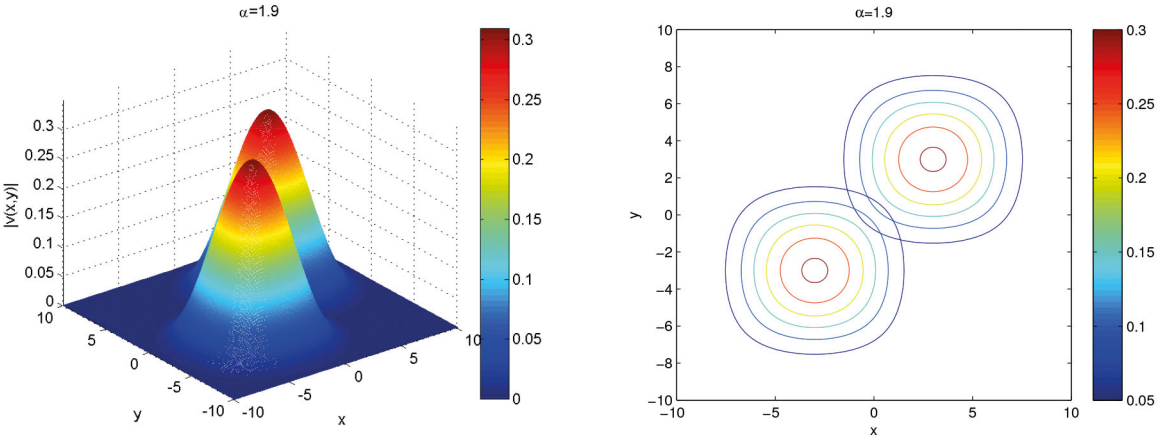

Fig. 13. Profile (left) and contour plot (right) of $|u|$ and $|v|$ for $\alpha = 1.9$.

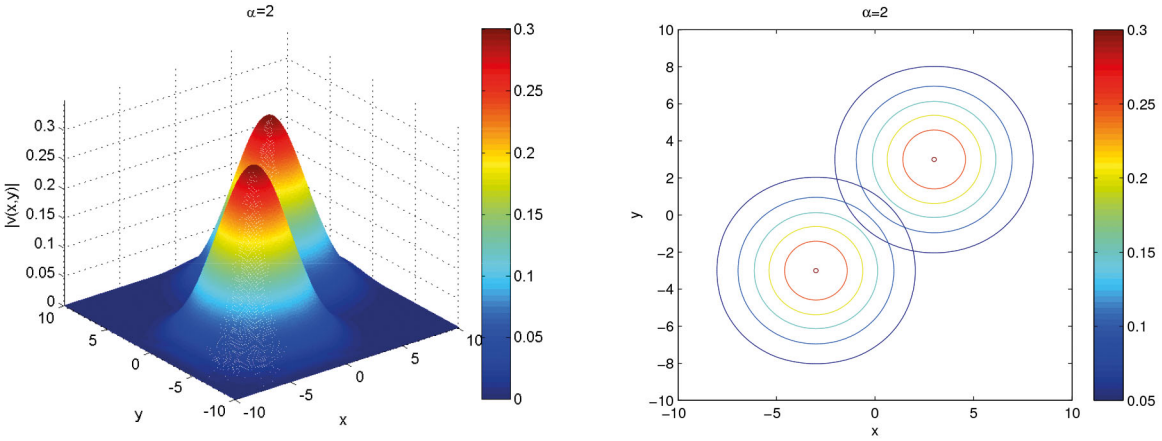

Fig. 14. Profile (left) and contour plot (right) of $|u|$ and $|v|$ for $\alpha = 2.0$.

8 Conclusion

In this paper, we proposed and analyzed the quasi-compact split-step finite difference methods for the one- and two-dimensional coupled fractional Schrödinger equations. For the linear problem, the conservation laws, prior boundedness estimates and unconditional error estimates of the resulting schemes are proved rigorously. Moreover, for the nonlinear problem, we showed that the quasi-compact SSFD scheme can keep the conservation law in the mass sense. Then, the quasi-compact split-step method and the ADI technique were combined together for solving the multi-dimensional problem. At last, numerical examples conformed our theoretical results and showed the efficiency of the proposed schemes.

This work was supported by NSF of China (No. 11701522, 11771163, 11671160), Henan Provincial Science and Technology Department Project (No. 19A110034) and China Postdoctoral Science Foundation (No. 2018M632791).

Appendix A. Some other schemes

For comparison, we introduce other three difference schemes in two dimensions. The first one is the quasi-compact Crank-Nicolson (QCCN) scheme

$$
\begin{aligned}
&i\mathcal{A}_x^\alpha\mathcal{A}_y^\alpha\delta_t u_{i,j}^{n+\frac{1}{2}}-\kappa\left[\mathcal{A}_y^\alpha\Delta_{h_x}^\alpha u_{i,j}^{n+\frac{1}{2}}+\mathcal{A}_x^\alpha\Delta_{h_y}^\alpha u_{i,j}^{n+\frac{1}{2}}\right]+\mathcal{A}_x^\alpha\mathcal{A}_y^\alpha\left[\frac{\rho}{2}\left(|u_{i,j}^{n+1}|^2+|u_{i,j}^{n}|^2+\beta|v_{i,j}^{n+1}|^2+\beta|v_{i,j}^{n}|^2\right)u_{i,j}^{n+\frac{1}{2}}\right]=0,\\
&(i,j)\in\mathcal{T}_{M_1\times M_2},\quad 1\le n\le N-1,\\
&i\mathcal{A}_x^\alpha\mathcal{A}_y^\alpha\delta_t v_{i,j}^{n+\frac{1}{2}}-\kappa\left[\mathcal{A}_y^\alpha\Delta_{h_x}^\alpha v_{i,j}^{n+\frac{1}{2}}+\mathcal{A}_x^\alpha\Delta_{h_y}^\alpha v_{i,j}^{n+\frac{1}{2}}\right]+\mathcal{A}_x^\alpha\mathcal{A}_y^\alpha\left[\frac{\rho}{2}\left(|v_{i,j}^{n+1}|^2+|v_{i,j}^{n}|^2+\beta|u_{i,j}^{n+1}|^2+\beta|u_{i,j}^{n}|^2\right)v_{i,j}^{n+\frac{1}{2}}\right]=0,\\
&(i,j)\in\mathcal{T}_{M_1\times M_2},\quad 1\le n\le N-1,\\
&u_{i,j}^0=u_0(x_i,y_j),\quad v_{i,j}^0=v_0(x_i,y_j),\quad (i,j)\in\mathbb{Z}^2,\\
&u_{i,j}^n=0,\quad v_{i,j}^n=0,\quad (i,j)\in\mathbb{Z}^2\backslash\mathcal{T}_{M_1\times M_2},\quad 1\le n\le N.
\end{aligned}
$$

The second one is the quasi-compact implicit midpoint (QCIM) scheme

$$
\begin{aligned}
&i\mathcal{A}_x^\alpha\mathcal{A}_y^\alpha\delta_t u_{i,j}^{n+\frac{1}{2}}-\kappa\left[\mathcal{A}_y^\alpha\Delta_{h_x}^\alpha u_{i,j}^{n+\frac{1}{2}}+\mathcal{A}_x^\alpha\Delta_{h_y}^\alpha u_{i,j}^{n+\frac{1}{2}}\right]+\mathcal{A}_x^\alpha\mathcal{A}_y^\alpha\left[\rho\left(|u_{i,j}^{n+\frac{1}{2}}|^2+\beta|v_{i,j}^{n+\frac{1}{2}}|^2\right)u_{i,j}^{n+\frac{1}{2}}\right]=0,\\
&(i,j)\in\mathcal{T}_{M_1\times M_2},\quad 1\le n\le N-1,\\
&i\mathcal{A}_x^\alpha\mathcal{A}_y^\alpha\delta_t v_{i,j}^{n+\frac{1}{2}}-\kappa\left[\mathcal{A}_y^\alpha\Delta_{h_x}^\alpha v_{i,j}^{n+\frac{1}{2}}+\mathcal{A}_x^\alpha\Delta_{h_y}^\alpha v_{i,j}^{n+\frac{1}{2}}\right]+\mathcal{A}_x^\alpha\mathcal{A}_y^\alpha\left[\rho\left(|v_{i,j}^{n+\frac{1}{2}}|^2+\beta|u_{i,j}^{n+\frac{1}{2}}|^2\right)v_{i,j}^{n+\frac{1}{2}}\right]=0,\\
&(i,j)\in\mathcal{T}_{M_1\times M_2},\quad 1\le n\le N-1,\\
&u_{i,j}^0=u_0(x_i,y_j),\quad v_{i,j}^0=v_0(x_i,y_j),\quad (i,j)\in\mathbb{Z}^2,\\
&u_{i,j}^n=0,\quad v_{i,j}^n=0,\quad (i,j)\in\mathbb{Z}^2\backslash\mathcal{T}_{M_1\times M_2},\quad 1\le n\le N.
\end{aligned}
$$

The last one is the quasi-compact linearly implicit (QCLI) scheme

$$
\begin{aligned}
&i\mathcal{A}_x^\alpha\mathcal{A}_y^\alpha\delta_{\hat{t}} u_{i,j}^{n}-\kappa\left[\mathcal{A}_y^\alpha\Delta_{h_x}^\alpha \hat{u}_{i,j}^{n}+\mathcal{A}_x^\alpha\Delta_{h_y}^\alpha \hat{u}_{i,j}^{n}\right]+\mathcal{A}_x^\alpha\mathcal{A}_y^\alpha\left[\rho\left(|u_{i,j}^{n}|^2+\beta|v_{i,j}^{n}|^2\right)\hat{u}_{i,j}^{n}\right]=0,\\
&(i,j)\in\mathcal{T}_{M_1\times M_2},\quad 1\le n\le N-1,\\
&i\mathcal{A}_x^\alpha\mathcal{A}_y^\alpha\delta_{\hat{t}} v_{i,j}^{n}-\kappa\left[\mathcal{A}_y^\alpha\Delta_{h_x}^\alpha \hat{v}_{i,j}^{n}+\mathcal{A}_x^\alpha\Delta_{h_y}^\alpha \hat{v}_{i,j}^{n}\right]+\mathcal{A}_x^\alpha\mathcal{A}_y^\alpha\left[\rho\left(|v_{i,j}^{n}|^2+\beta|u_{i,j}^{n}|^2\right)\hat{v}_{i,j}^{n}\right]=0,\\
&(i,j)\in\mathcal{T}_{M_1\times M_2},\quad 1\le n\le N-1,\\
&u_{i,j}^0=u_0(x_i,y_j),\quad v_{i,j}^0=v_0(x_i,y_j),\quad (i,j)\in\mathbb{Z}^2,\\
&u_{i,j}^n=0,\quad v_{i,j}^n=0,\quad (i,j)\in\mathbb{Z}^2\backslash\mathcal{T}_{M_1\times M_2},\quad 1\le n\le N,
\end{aligned}
$$

where $\delta_{\hat{t}}u_{i,j}^n=(u_{i,j}^{n+1}-u_{i,j}^{n-1})/(2\tau)$ and $\hat{u}_{i,j}^n=(u_{i,j}^{n+1}+u_{i,j}^{n-1})/2$.

In order to implement the numerical experiments, the efficient iterative algorithms of the QCCN and QCIM schemes are also essential. See more details in [20–22,26]. Since a new coefficient matrix should be generated at each time step, the compute of the QCLI scheme is very expensive. An iteration procedure (QCLII) is also proposed as follows:

$$
\begin{aligned}
&i\mathcal{A}_x^\alpha\mathcal{A}_y^\alpha\frac{u_{i,j}^{n+1(s+1)}-u_{i,j}^{n-1}}{2\tau}-\frac{\kappa}{2}\left[\mathcal{A}_y^\alpha\Delta_{h_x}^\alpha(u_{i,j}^{n+1(s+1)}+u_{i,j}^{n-1})+\mathcal{A}_x^\alpha\Delta_{h_y}^\alpha(u_{i,j}^{n+1(s+1)}+u_{i,j}^{n-1})\right]\\
&+\mathcal{A}_x^\alpha\mathcal{A}_y^\alpha\left[\frac{\rho}{2}\left(|u_{i,j}^n|^2+\beta|v_{i,j}^n|^2\right)(u_{i,j}^{n+1(s)}+u_{i,j}^{n-1})\right]=0,\quad (i,j)\in\mathcal{T}_{M_1\times M_2},\quad 1\le n\le N-1,\quad s=0,1,2\cdots,\\
&i\mathcal{A}_x^\alpha\mathcal{A}_y^\alpha\frac{v_{i,j}^{n+1(s+1)}-v_{i,j}^{n-1}}{2\tau}-\frac{\kappa}{2}\left[\mathcal{A}_y^\alpha\Delta_{h_x}^\alpha(v_{i,j}^{n+1(s+1)}+v_{i,j}^{n-1})+\mathcal{A}_x^\alpha\Delta_{h_y}^\alpha(v_{i,j}^{n+1(s+1)}+v_{i,j}^{n-1})\right]\\
&+\mathcal{A}_x^\alpha\mathcal{A}_y^\alpha\left[\frac{\rho}{2}\left(|v_{i,j}^n|^2+\beta|u_{i,j}^n|^2\right)(v_{i,j}^{n+1(s)}+v_{i,j}^{n-1})\right]=0,\quad (i,j)\in\mathcal{T}_{M_1\times M_2},\quad 1\le n\le N-1,\quad s=0,1,2\cdots,\\
&u_{i,j}^0=u_0(x_i,y_j),\quad v_{i,j}^0=v_0(x_i,y_j),\quad (i,j)\in\mathbb{Z}^2,\\
&u_{i,j}^n=0,\quad v_{i,j}^n=0,\quad (i,j)\in\mathbb{Z}^2\backslash\mathcal{T}_{M_1\times M_2},\quad 1\le n\le N,
\end{aligned}
$$

where

$$u_{i,j}^{n+1(s)}=2u_{i,j}^n-u_{i,j}^{n-1},\quad v_{i,j}^{n+1(s)}=2v_{i,j}^n-v_{i,j}^{n-1},\quad 1\le n\le N-1.$$

References

1. N. Laskin, Phys. Rev. E **62**, 3135 (2000).
2. N. Laskin, Phys. Rev. E **66**, 056108 (2002).
3. M. Naber, J. Math. Phys. **45**, 3339 (2004).
4. X. Guo, M. Xu, J. Math. Phys. **47**, 082104 (2006).
5. B. Stickler, Phys. Rev. E **88**, 012120 (2013).
6. S. Longhi, Opt. Lett. **40**, 1117 (2015).
7. R. Herrmann, arXiv:0805.3434.
8. W. Chen, J. Vib. Control **14**, 1651 (2008).
9. N.C. Petroni, M. Pusterla, Physica A **388**, 824 (2009).
10. S. Secchi, arXiv:1208.2545.
11. S. Secchi, M. Squassina, Appl. Anal. **93**, 1702 (2014).
12. B. Guo, Y. Han, J. Xin, Appl. Math. Comput. **204**, 468 (2008).
13. Y. Hu, G. Kallianpur, Appl. Math. Optim. **42**, 281 (2000).
14. P. Amore, F.M. Fernández, C.P. Hofmann, R.A. Sáenz, J. Math. Phys. **51**, 122101 (2010).
15. W. Bao, X. Dong, J. Comput. Phys. **230**, 5449 (2011).
16. A. Atangana, A.H. Cloot, Adv. Differ. Equ. **2013**, 80 (2013).
17. L. Wei, Y. He, X. Zhang, S. Wang, Finite Elem. Anal. Des. **59**, 28 (2012).
18. L. Wei, X. Zhang, S. Kumar, A. Yildirim, Comput. Math. Appl. **64**, 2603 (2012).
19. X. Zhao, Z.-z. Sun, Z.-p. Hao, SIAM J. Sci. Comput. **36**, 2865 (2014).
20. D. Wang, A. Xiao, W. Yang, J. Comput. Phys. **242**, 670 (2013).
21. D. Wang, A. Xiao, W. Yang, J. Comput. Phys. **272**, 644 (2014).
22. D. Wang, A. Xiao, W. Yang, Appl. Math. Comput. **257**, 241 (2015).
23. P. Wang, C. Huang, J. Comput. Phys. **293**, 238 (2015).
24. P. Wang, C. Huang, Numer. Algorithms **69**, 625 (2015).
25. P. Wang, C. Huang, L. Zhao, J. Comput. Appl. Math. **306**, 231 (2016).
26. P. Wang, C. Huang, Comput. Math. Appl. **71**, 1114 (2016).
27. M. Li, C. Huang, P. Wang, Numer. Algorithms **74**, 499 (2016).
28. M. Li, C. Huang, W. Ming, Numer. Algorithms (2019) `https://doi.org/10.1007/s11075-019-00672-3`.
29. M. Li, X.-M. Gu, C. Huang, M. Fei, G. Zhang, J. Comput. Phys. **358**, 256 (2018).
30. M. Li, Y.-L. Zhao, Appl. Math. Comput. **338**, 758 (2018).
31. A. Bhrawy, M. Zaky, Appl. Numer. Math. **111**, 197 (2017).
32. M. Dehghan, M. Abbaszadeh, W. Deng, Appl. Math. Lett. **73**, 120 (2017).
33. M. Dehghan, M. Abbaszadeh, A. Mohebbi, J. Comput. Appl. Math. **280**, 14 (2015).
34. M. Dehghan, M. Abbaszadeh, Appl. Numer. Math. **119**, 51 (2017).
35. M. Dehghan, M. Abbaszadeh, Appl. Numer. Math. **131**, 190 (2018).
36. M. Dehghan, J. Manafian, A. Saadatmandi, Numer. Methods Part. Differ. Equ. **26**, 448 (2010).
37. M. Li, C. Huang, Numer. Methods Part. Differ. Equ. (2019) `https://doi.org/10.1002/num.22305`.
38. M. Dehghan, M. Safarpoor, Math. Methods Appl. Sci. **39**, 2461 (2016).
39. A. Taleei, M. Dehghan, Comput. Phys. Commun. **185**, 1515 (2014).

40. A. Mohebbi, M. Abbaszadeh, M. Dehghan, Eng. Anal. Bound. Elem. **37**, 475 (2013).
41. J. Weideman, B. Herbst, SIAM J. Numer. Anal. **23**, 485 (1986).
42. G. Muslu, H. Erbay, Math. Comput. Simul. **67**, 581 (2005).
43. H. Wang, Appl. Math. Comput. **170**, 17 (2005).
44. T.R. Taha, X. Xu, J. Supercomput. **32**, 5 (2005).
45. M. Dehghan, A. Taleei, Comput. Phys. Commun. **181**, 43 (2010).
46. X. Antoine, W. Bao, C. Besse, Comput. Phys. Commun. **184**, 2621 (2013).
47. Y. Ma, L. Kong, J. Hong, Y. Cao, Comput. Math. Appl. **61**, 319 (2011).
48. L. Kong, J. Hong, L. Ji, P. Zhu, Numer. Methods Part. Differ. Equ. **31**, 1814 (2015).
49. C. Chen, J. Hong, L. Ji, L. Kong, Commun. Comput. Phys. **21**, 93 (2017).
50. S. Duo, Y. Zhang, Comput. Math. Appl. **71**, 2257 (2016).
51. N. Wang, C. Huang, Comput. Math. Appl. **75**, 2223 (2018).
52. K. Kirkpatrick, E. Lenzmann, G. Staffilani, Commun. Math. Phys. **317**, 563 (2013).
53. Z. Fei, V.M. Pérez-Garcia, L. Vázquez, Appl. Math. Comput. **71**, 165 (1995).
54. S. Li, L. Vu-Quoc, SIAM J. Numer. Anal. **32**, 1839 (1995).
55. Z. Yang, Int. J. Comput. Math. **93**, 609 (2016).
56. M.M. Meerschaert, C. Tadjeran, J. Comput. Appl. Math. **172**, 65 (2004).
57. M.M. Meerschaert, C. Tadjeran, Appl. Numer. Math. **56**, 80 (2006).
58. W. Tian, H. Zhou, W. Deng, Math. Comput. **84**, 1703 (2015).
59. H. Zhou, W. Tian, W. Deng, J. Sci. Comput. **56**, 45 (2013).
60. M. Chen, W. Deng, SIAM J. Numer. Anal. **52**, 1418 (2014).
61. M. Chen, W. Deng, Commun. Comput. Phys. **16**, 516 (2014).
62. H. Ding, C. Li, Y. Chen, J. Comput. Phys. **293**, 218 (2015).
63. Z.-p. Hao, Z.-z. Sun, W.-r. Cao, J. Comput. Phys. **281**, 787 (2015).
64. P. Wang, C. Huang, J. Comput. Phys. **312**, 31 (2016).
65. L. Trefethen, *Spectral Methods in MATLAB*, Vol. **10** (SIAM, Philadelphia, 2000).
66. J. Strikwerda, *Finite Difference Schemes and Partial Differential Equations* (SIAM, Philadelphia, 2004).
67. Q. Du, M. Gunzburger, R.B. Lehoucq, K. Zhou, SIAM Rev. **54**, 667 (2012).
68. O. Defterli, M. D'Elia, Q. Du, M. Gunzburger, R. Lehoucq, M.M. Meerschaert, Fract. Calc. Appl. Anal. **18**, 342 (2015).